Geophysical Methods for Investigating Ground-Water Recharge

By Ty P.A. Ferré[1], Andrew M. Binley[2], Kyle W. Blasch, James B. Callegary, Steven M. Crawford, James B. Fink[3], Alan L. Flint, Lorraine E. Flint, John P. Hoffmann, John A. Izbicki, Marc T. Levitt[3], Donald R. Pool, and Bridget R. Scanlon[4]

Introduction

Numerical models of water flow have revolutionized our understanding of basin-scale hydrologic processes. To date, these models have relied primarily on traditional hydrologic monitoring—of rainfall, streamflow, and water-table elevations, for example—for calibration and performance testing. Calibration provides initial estimates of the rates and distribution of ground-water recharge, and the calibrated models that result provide important tools for addressing recharge questions. This inverse approach has been preferred over monitoring of recharge due to the inherent difficulties of making direct measurements of flow across the water table. The difficulty is magnified because recharge fluxes are typically small and because the location of the water table changes with time. In arid and semiarid regions, deep water tables make recharge monitoring especially challenging. Despite the challenges, recharge monitoring must advance to allow for continued improvement in our understanding of basin-scale hydrologic processes. Such understanding is crucial for future water resource characterization and planning.

The difficulties associated with measuring recharge directly have led to growing interest in the adoption and development of indirect methods to measure or estimate recharge. The mass balance approach of estimating recharge as the residual of other (generally larger) terms has advanced through the use of more complex and more complete basin-scale hydrologic models. Improved measurements of recharge rates, timing, and patterns can be used to improve these modeling efforts by providing boundary conditions, constraints on model inputs, data for the testing of simplifying assumptions, and identification of spatial and temporal resolution of model inputs necessary to predict recharge to specified tolerances in space and in time. Under some conditions, improved measurements may provide a direct measure of recharge or changes in water storage, largely eliminating the need for indirect estimates of recharge.

This appendix presents an overview of physically based, indirect, geophysical methods that are available or in development for recharge monitoring. The material is written primarily for hydrologists. It is not intended to be an exhaustive review of geophysical methods; rather, the intent is to introduce the possible uses of geophysical methods for improved recharge monitoring through brief discussions and case studies. The focus is to present an approach to determine how geophysical methods can be used most effectively in quantifying recharge and studying recharge processes. As such, it is presented as a conceptual framework for matching the strengths of individual geophysical methods with the manners in which they can be applied for hydrologic analyses. For further information on individual geophysical methods, readers are referred to excellent texts describing the theory and practice of geophysics including Telford and others (1990) and Reynolds (1997). A 2002 workshop on advanced hydrogeophysics led to a well-organized collection of papers describing classical concepts and emerging techniques (Rubin and Hubbard, 2005). An illustrated introduction to the geophysical techniques most commonly used in alluvial deposit characterization appears in a recent USGS circular (Lucius and others, 2007).

This appendix is organized in three sections. First, the key hydrologic parameters necessary to determine the rates, timing, and patterns of recharge are identified. Second, the basic operating principals of selected geophysical methods are presented. The methods are grouped by the physical property that they measure directly (table 1). Each measured property is related to one or more of the key hydrologic properties for recharge monitoring. Third, the emerging conceptual framework for applying geophysics to recharge monitoring is summarized in the closing remarks.

Examples of the application of selected geophysical methods to recharge monitoring are presented in sidebars. These case studies illustrate hydrogeophysical applications under a range of conditions and measurement scales, which vary from tenths of a meter to hundreds of meters (table 1).

[1]Department of Hydrology and Water Resources, University of Arizona, Tucson, Arizona (ty@hwr.arizona.edu).

[2] Department of Environmental Science, Lancaster University, Lancaster, United Kingdom (A.Binley@lancaster.ac.uk).

[3] hydroGEOPHYSICS Inc., Tucson, Arizona (mail@hydrogeophysics.com).

[4]Jackson School of Geosciences, University of Texas at Austin, Austin, Texas (Bridget.Scanlon@beg.utexas.edu).

Table 1. Geophysical methods available or in development for recharge monitoring—comparison of directly measured properties or parameters, approximate measurement scales, and primary applications (×).

Method	Measured property or parameter	Measurement scale (meters)	Primary recharge monitoring application(s)			
			Hydrogeologic framework	Water mass balance	Direct flux measurement	Vadose zone model calibration
Seismic	Seismic velocity	10s–100s	×			
Time-domain reflectometry (TDR)	Dielectric permittivity	0.1–1				×
Time-domain transmission (TDT)	ditto	0.1–1				×
Ground penetrating radar (GPR)	ditto	1–10	×	×		×
Capacitance	ditto	0.1–1				×
Electrical resistance tomography (ERT)	Electrical conductivity	10s–100s	×	×		×
Electromagnetic induction (EMI)	ditto	1–10s	×	×		×
Time-domain electromagnetics (TEM)	ditto	10s–100s	×	×		×
Streaming potential (SP)	ditto	10s–100s			×	
Controlled source audio magnetotellurics (CSAMT)	ditto	10s–100s	×			
Nuclear magnetic resonance (NMR)	Proton precession	10s–100s	×	×		×
Gravity	Mass change	10s–100s	×	×		
Neutron	Hydrogen density	0.1–1	×	×		×
Temperature[1]	Temperature	1–10s			×	×

[1]Temperature methods are discussed in appendix 1 of this volume.

In addition, case studies have been selected to show practice-proven as well as recently emerging applications of geophysical methods to recharge monitoring. Because these recent applications have received testing in relatively few locations, the case studies on emerging techniques involve applications relatively far from the study area—including one in the United Kingdom and one in south-central Washington State.

Key Hydrologic Parameters for Recharge Monitoring

Recharge in granular media can be identified in one of three ways: (1) changes in water storage in the saturated zone can be measured and attributed to recharge, (2) the water flux past a fixed depth can be measured and equated to recharge, or (3) calibrated numerical variably saturated water-flow models can be constructed and used to infer the rates and patterns of water movement throughout the subsurface. Each of these approaches to recharge characterization is discussed briefly to give a context for considering the use of geophysical methods for recharge estimation. Note that this appendix is limited to the topic of recharge in unconfined, granular media. At this time, quantitative application of geophysical methods to monitoring recharge in fractured media or to confined aquifers is limited.

Monitoring Changes in Water Storage in the Saturated Zone

Changes in water storage in the subsurface occur due to the following processes: natural and artificial infiltration at the ground surface, evapotranspiration, lateral inflow and outflow, and withdrawal or addition from pumping wells and injection wells. Typically, basin-scale hydrologic models lump the processes of infiltration, evapotranspiration, and redistribution within the unsaturated zone, expressing the net result as a recharge flux across the water table. Subsurface water flow is then treated by only considering water flow through a saturated medium. If water withdrawals by pumping, inflows/outflows, and the storage characteristics of the medium near the

water table are well-characterized, then spatial and temporal changes in the water table elevation can be used to constrain a saturated flow model to infer the rates, patterns, and timing of recharge. This can be simplified further by ignoring the rates of inflow and outflow and equating measured changes in water table elevation with recharge. This simple approach, while lacking the explanatory capabilities of a calibrated flow numerical model, is particularly useful for rapid water-resource evaluation. More complex basin-scale analyses may rely on calibrated saturated-flow numerical models. However, these also have limited predictive capabilities because they do not explicitly represent unsaturated zone processes. As a result, these models should only be applied for recharge prediction under climatic conditions that are similar to those used for model calibration.

Numerical saturated-flow models are usually calibrated by using measurements of water-table elevation or estimates of subsurface storage within the basin. These models also require estimates of inflow and outflow across the boundaries. To relate the timing and patterns of water table elevation change to the rates, timing, and patterns of recharge, the distribution of hydraulic properties also must be defined throughout the domain. The key properties that control the accuracy of recharge estimation based on saturated-flow numerical modeling are hydraulic property distributions, the water flux across the water table, and the water content or pressure head change in the vicinity of the water table.

Monitoring Water Flux over a Fixed-Depth Interval

Recharge to an unconfined aquifer is defined as the positive downward flux across the water table. Therefore, measurements of water flux at the water table provide the only direct measure of recharge. Direct recharge monitoring may be possible at a limited number of sites within a well-instrumented watershed with relatively shallow water tables. However, given that the water-table elevation changes in time, it is more practical to conceive of measurements that are made at some fixed depth (or depths) either above the water table or spanning the water table. The closer the measurement depth is to the water table, the more faithfully the measured or inferred flux will represent the recharge flux, both in magnitude and in timing. However, shallower measurements are typically less expensive, with the least costly measurements being remote sensing of ground surface. These reduced costs translate to greater spatial coverage. As a result, flux monitoring over a fixed depth interval is a balance between relatively sparse measurements of the local recharge flux versus greater spatial coverage of the water flux at some point at a shallower depth within the unsaturated zone. As with the saturated-zone modeling approach described above, fixed-depth interval monitoring requires significant simplifying assumptions regarding flow processes within the unsaturated zone. Therefore, these measurements cannot be used to link surface and unsaturated-zone processes with the timing and pattern of recharge. Rather, this approach provides either improved estimates of the local recharge flux (by using deep measurements), or improved spatial representation of water fluxes within the unsaturated zone (by using shallow measurements) when compared to saturated-flow numerical models. As a result, fixed-depth interval monitoring is amenable to both water-resource planning and to some large-scale scientific analyses.

Fixed-depth interval flux monitoring can be applied to either transient or steady-state infiltration and recharge. Monitoring transient infiltration processes can take advantage of changes in water content that are associated with transient flow through unsaturated media. During the advance of a wetting front, changes in the volume (or length, in one dimension) of water between the wetting front and the ground surface can be related directly to changes in the volume (or length) of water stored in the unsaturated zone. Simultaneous volumetric water-content measurements throughout the unsaturated zone can be used to determine directly the volume (or length) of water stored. Changes in the water stored with time can be related to the cumulative net infiltration (infiltration less evapotranspiration) until the wetting front reaches a zone of full saturation. Alternatively, water-content or pressure-head measurements made at specific points can be used to constrain unsaturated-flow models to infer the flux past the deepest observation point as a function of time. Inference of the flux using this approach requires characterization of the unsaturated hydraulic properties throughout the zone of measurement. Monitoring steady-state infiltration and recharge is more challenging. Under steady-state conditions, there is no change in water content associated with infiltration. As a result, steady-state flux can only be estimated by using direct measurements of water flux at a fixed depth, or by measuring vertical pressure-head gradients and calculating flux from known hydraulic conductivity functions for the site materials. Alternatively, the water velocity can be measured and related to the water flux through the measured volumetric water content.

Characterizing Water Flow throughout the Unsaturated Zone

Full characterization of the rates, timing, and patterns of recharge requires complete analysis of water movement throughout the unsaturated zone. Ideally, this analysis would be conducted by using a multidimensional numerical model that accounts for liquid and vapor movement, preferential flow, and root uptake, among other processes. In addition, the subsurface hydraulic property distribution would be characterized with high spatial resolution throughout the domain. Such a model could then be calibrated by using measurements of water content and water pressure at multiple depths, at many times, and at many locations throughout a basin. This well-calibrated model could then be used to infer recharge rates

and to predict the impact of processes at the ground surface and throughout the unsaturated zone on recharge rates, timing, and patterns. It is impractical to construct and calibrate such a model for each basin of interest. Rather, these models can be used to improve our understanding of the dependences of fluxes at fixed depths and changes in water storage on processes that occur at the ground surface and throughout the unsaturated zone. These insights can then be used to improve recharge analyses based on saturated-flow models or flux measurements made at limited depths. For example, it would be useful to identify and characterize the systematic errors of these simpler approaches and to determine the conditions for which they can be used with acceptable error or uncertainly of recharge estimates. Similarly, more complete models of water flow throughout the unsaturated zone could be used to design a monitoring network that combines measurements within the saturated zone and at selected locations within the unsaturated zone to produce the most accurate recharge estimates within an available budget. Stochastic approaches may play a key role in characterizing the uncertainty of recharge estimates and in identifying optimal monitoring networks for specific applications (for example, Yeh and Simunek, 2002).

Geophysical Methods for Recharge Monitoring—Principles

Four key hydrologic parameters for recharge monitoring have been identified: hydraulic property distributions in space, water content distributions in space and time, water pressure distributions in space and time, and water flux distributions in space and time. To date, geophysical methods have only seen limited use in direct measurement and monitoring of water flow in the subsurface. More commonly, geophysics fills its traditional role of characterization of subsurface hydrologic properties either by using surface-based methods or borehole methods. This role can be expanded and improved through the routine incorporation of geophysical data in constructing domains for numerical models of water flow. However, this will likely require new approaches to the interpretation and application of geophysical methods to highlight the heterogeneity and anisotropy of hydraulic conductivity that are of particular importance to hydrologic investigations. Similarly, expanded use of geophysics for flux monitoring will require new approaches to geophysical survey design and geophysical data interpretation that are aimed specifically at hydrologic applications. Furthermore, improvements in the application and interpretation of geophysical data for hydrologic applications must be made with consideration of the scales of measurement and the costs of geophysical surveys. For the near future, the use of geophysics for hydrologic monitoring will expand only if there are clear cost savings or significantly improved framework data that balance the added costs. As a result, the conceptual framework for the application of geophysical methods to recharge monitoring presented here is focused on practically achievable contributions that likely can be made by geophysics within the next decade rather than on the eventual possibilities of geophysical monitoring.

Geophysical methods vary widely in their physical bases and methods of application. However, the expected contributions of geophysical methods to recharge monitoring can be assessed based on three common factors: the sensitivity of the instrument response to changes in hydrologically relevant properties, the ability of the method to provide measurements with sufficient spatial and temporal resolutions to characterize hydrologically relevant properties, and practical limitations to field applications of the method. In this section, geophysical methods are introduced that are currently available or in late-stage development for recharge monitoring. The methods are grouped by the physical property measured, seismic velocity, dielectric permittivity, electrical conductivity, proton precession, mass change, hydrogen density, or temperature. Each physical property is related to hydrologically relevant properties. Then, the physical basis of each method is presented. Finally, the resolution and applicability of each method for recharge monitoring are discussed. Case studies demonstrating the application of selected geophysical methods to recharge monitoring are shown as illustrative sidebars. To highlight geophysical methods, traditional hydrologic methods such as thermogravimetric soil water content measurement, piezometry, and tensiometry are not discussed. Readers are encouraged to refer to complete texts such as Methods of Soils Analysis (Dane and Topp, 2002) for more complete discussion of these methods. In addition, some methods that can contribute to recharge studies exclusively through geologic mapping (for example, geomagnetic methods) are not discussed here—only seismic methods are presented for structural geologic characterization. Finally, temperature methods, which have seen great recent success in recharge monitoring, are not discussed here because they are presented in detail in appendix 1.

Seismic Velocity

The density and elastic properties of a porous medium control the speed with which seismic waves will propagate through the medium, which is known as the seismic velocity of the medium (with units of length divided by time). Specifically, the seismic velocity of a medium is directly related to the square root of the ratio of the elastic modulus to the density. That is, increased rigidity and decreased density lead to an increased seismic velocity. The seismic velocities in air and water are 0.35 kilometers per second (km/s) and 1.5 km/s, respectively. The seismic velocity in rocks ranges from 1.75 km/s in porous shale to more than 7 km/s in low porosity dolomite (Birch, 1966). The seismic velocity in a partially saturated porous medium increases with increasing water content. This increase is a balance of the effects of the higher velocity of propagation through water filled pores and the increased density due to water displacing air within the medium. Similarly, seismic velocity decreases in a linear fashion as oil replaces water in a porous medium (Geller and Myer, 1995).

Kohnen (1974) reported seismic velocities ranging from 0.2 to 2 km/s in sands variably saturated with air and water.

Because the seismic velocity depends on both the elastic properties and density of the solid matrix and the volumetric water content, it would appear that this method could be used to map water content distributions as well as hydrogeologic structure. Time-lapse seismic monitoring of water-content change has been applied successfully at the laboratory scale (for example, Geller and Myer, 1995). However, the typical mode of application of seismic methods at the field scale precludes water content mapping. Specifically, seismic methods are typically operated in reflection or refraction mode wherein a seismic source is activated, commonly at or near the ground surface, and seismic waves are recorded with time at or near the ground surface. Seismic energy travels along multiple paths including a direct path between the source and receiver and indirect paths of reflected and refracted rays. Direct arrivals can potentially be useful for characterizing the seismic velocity between the source and receiver. The simultaneous inversion of data recorded from multiple source and receiver locations within boreholes can potentially be used to construct a two- or three-dimensional image of the velocity distribution. This might then be used, together with supporting information, to characterize the water-content distribution. However, current field applications rarely use multiple down-hole source and recording positions, primarily due to difficulties with coupling the source and receivers to the medium within the unsaturated zone. It is far more common to conduct surveys at the ground surface and to interpret structure based on reflected or refracted energy. This survey approach relies on sharp changes in the seismic velocity in the subsurface to give rise to reflections and refractions. The responses from these different travel paths can be separated on a seismograph due to their different travel path lengths and propagation velocities. However, this typically requires that seismic surveys be applied at scales of meters to tens of meters between measurement points. This scale of application, together with the relatively large minimum resolvable bed thicknesses achievable with seismic waves, limits the ability of seismic methods to characterize water content distributions with sufficient resolution to constrain unsaturated water flow models. As a result, high-resolution applications of seismic methods for water content mapping will likely remain limited to the laboratory for the near future. While the relatively large measurement scale of seismic methods is a limitation for water content mapping, it is an advantage for defining the hydrogeologic structure of relatively deep unsaturated zones. Hydraulic and physical properties often most commonly obtained from drill cuttings and cores; however, these data typically are sparse owing to their associated costs and, thus, are limited in defining the geometry of subsurface deposits. Seismic data can be used to extend the limited hydraulic and physical properties of the shallow subsurface sediments and to define vertical and lateral extents of subsurface layers. An example of this application is shown in the sidebar "Estimating stream-channel deposit geometry with seismic-refraction surveys." The ready availability of seismic instruments and the wealth of expertise in the use and interpretation of seismic methods from the minerals and petroleum exploration industries suggest that the use of seismic methods should be a standard for the definition of hydrogeologic structure for basin-scale hydrologic models. High-resolution seismic methods may also contribute to the definition of hydrologic structure for detailed models of water flow throughout the unsaturated zone.

Dielectric Permittivity

The dielectric permittivity (farads per meter) describes the ability of a medium to store charge in an alternating electromagnetic field. In general, the bulk dielectric permittivity of a medium depends on the dielectric permittivities, electrical conductivities, and magnetic permeabilities of the constituents of the medium, weighted by their volume fractions. Furthermore, the dielectric permittivity depends upon the frequency of the applied electromagnetic field. Researchers are currently exploring the use of multifrequency analyses of complex dielectric permittivity measurements to infer soil-specific properties, such as mineral composition and water-air interfacial areas. However, most dielectric permittivity methods that will be applied to recharge monitoring in the near future operate in a frequency range over which the dielectric permittivity of water can be considered nearly independent of frequency. Furthermore, most of these applications will be conducted in nonmagnetic media, eliminating complications due to high magnetic permeability materials. Typically, dielectric methods applied to recharge studies will rely on determination of the apparent dielectric permittivity relative to the permittivity of a vacuum. Use of this dimensionless lumped parameter assumes that the imaginary component of the complex dielectric permittivity, which is related to conductive and dielectric losses, does not contribute significantly to the medium's dielectric response. With this assumption, the velocity of propagation of an electromagnetic wave can be related directly to the inverse of the square root of the relative apparent dielectric permittivity.

The bulk dielectric permittivity can be related to the dielectric permittivity of the soil components through variations of the complex refractive index model:

$$\sqrt{\kappa} = (1-\varphi)\sqrt{\kappa_s} + \theta\sqrt{\kappa_w} + (\varphi-\theta)\sqrt{\kappa_a} \quad , \qquad (1)$$

where

κ_s = the dielectric constant of the sediment grains,

κ_w = the dielectric constant of water (assumed to be 81),

θ = the volumetric water content, and

φ = the porosity.

The relatively high dielectric constant of water compared to other soil components imparts the strong dependence of the bulk dielectric permittivity on the volumetric water content of the medium. In fact, the bulk dielectric permittiv-

Estimating Stream-Channel Deposit Geometry with Seismic-Refraction Surveys

By John P. Hoffmann

The amount of water that recharges many aquifers in the Southwest is insufficient to meet current and future demands. As a result, water levels have declined tens of meters in the past several years. For instance, in the Tucson area, water levels have declined by as much as 60 meters over the past 50 years (Tucson Water, 2000). Many ephemeral streams in the Southwest, such as Rillito Creek, are being considered as artificial-recharge sites to help mitigate the deficit. Design and construction of in-channel recharge facilities, in the absence of information that can be used to estimate performance and optimize design, constitute an expensive and uncertain venture.

Infiltrated water within the Rillito Creek stream-channel deposits is a primary source of recharge for the alluvial aquifer underlying the city of Tucson and surrounding areas. Rillito Creek, located in Upper Santa Cruz Basin in southern Arizona, is typical of a large ephemeral-stream channel in the Southwest. In many of the Southwest basins, such as in Upper Santa Cruz Basin, streams originating at higher elevations coalesce downstream to form larger ephemeral streams. Streams originating near mountain fronts typically flow over thick alluvial valleys, lose hydraulic connection with the underlying aquifer, and become ephemeral in their lower reaches. Underlying many of these ephemeral streams is a coarse-grained stream-channel deposit that overlies a basin-fill deposit. The coarse-grained stream-channel deposit typically has high permeability that enables high infiltration rates and provides storage capacity for subsequent ground-water recharge. In places, Rillito Creek has an unsaturated zone that is 40 meters thick (Hoffmann and others, 2002).

The stream-channel deposits are predominantly sand and gravel with less than 5 percent clay and silt, while the underlying basin-fill deposits are finer grained, typically having 10 percent or more of silt and clay (Hoffman and others, 2002). The difference in grain size between the deposits results in differing hydraulic and physical values for the deposits. For instance, the average hydraulic conductivity of the stream-channel deposits is about 1.2 meters per day (m/d), whereas the average hydraulic conductivity of the basin-fill deposit is 0.2 m/d. In addition, the field capacity of the stream-channel deposits is about 18 percent by volume and about 24 percent by volume in the basin-fill deposits. Porosity of both deposits is close to 30 percent. Given the hydraulic and physical differences between the deposits that underlie Rillito Creek, it is important to accurately characterize the geometry of these deposits to better estimate infiltration, storage, and subsequent recharge capacity of the sediments.

As part of an investigation of the hydrogeology of Rillito Creek, 51 core samples from five boreholes were collected and analyzed for hydraulic and physical properties (Hoffmann and

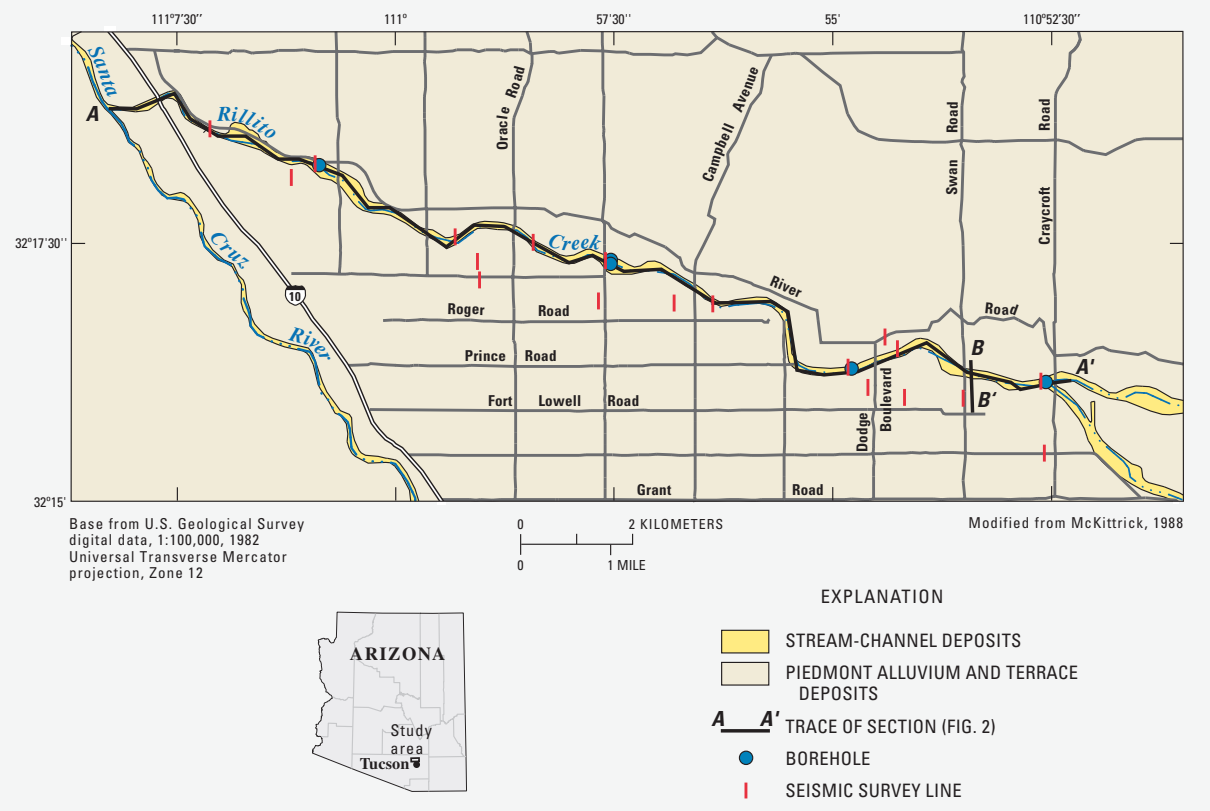

Figure 1. Location of study area showing borehole and seismic-survey locations, Rillito Creek, Pima County, Ariz.

others, 2002). In addition, seismic-refraction surveys were done at each borehole and at several intermediate locations between boreholes and on the adjacent stream-channel terrace. Twelve surveys were conducted within the stream channel along a 20-km reach and 12 surveys were conducted on the adjacent terrace deposits (fig. 1). Four of the in-channel surveys were near boreholes having geologic logs; therefore, the wells could be used as ground truth for the seismic surveys. Seismic-velocity values for the unsaturated recent stream alluvium averaged 400 m/s and ranged from 350 to 500 m/s, whereas the velocities for unsaturated basin-fill deposits averaged about 840 m/s and ranged from 600 to 1,400 m/s. In locations where the saturated zone was generally less than 10 m below ground surface, seismic-refraction surveys were capable of detecting the water table—seismic velocity values for the saturated basin-fill deposit averaged 2,400 m/s and ranged from 1,500 to 3,500 m/s. Thickness of stream-channel deposits estimated by the refraction surveys generally agreed with geologic logs at adjacent wells to within about a meter allowing for confident extension of the definition of the basin-fill contact. Thickness of the stream-channel deposits averaged approximately 7 m and ranged from 3 to 9 m along the 20-km reach (fig. 2*A*). Cross-channel surveys were used to estimate the width of the stream-channel deposit, such as shown in the cross section in figure 2*B*.

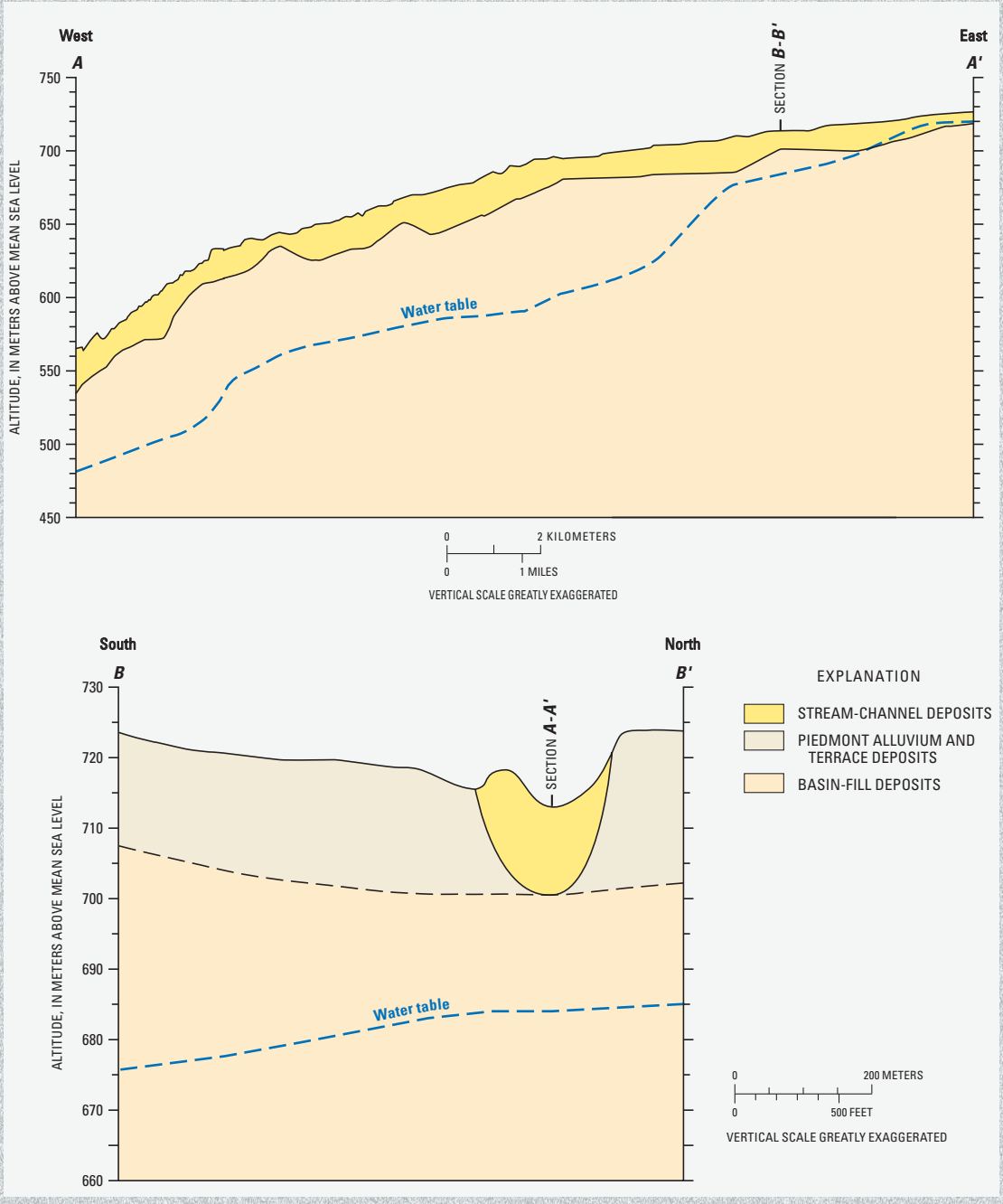

Figure 2. *A,* Section of longitudinal section based on seismic and borehole data; *B,* Cross-channel section based on seismic data, Rillito Creek, Pima County, Ariz.

ity of most unconsolidated geologic materials depends upon the volumetric water content with only minor dependence on the volume fraction or the composition of the solids or of the composition of the water and other pore fluids. As a result of this insensitivity to medium-specific properties, the volumetric water content can be determined with reasonable accuracy by using a general calibration equation, such as that presented by Topp and others (1980). Examining the change in bulk dielectric permittivity with time and relating this to the change in water content can reduce the dependence on the bulk dielectric permittivity of the soil solids further. While general relationships relating dielectric permittivity (change) and volumetric water content (change) can be applied under most conditions, two limitations must be considered. First, measurements in highly electrically conductive environments can lead to systematic measurement errors and increased measurement uncertainties (Hook and others, 2004). Second, clay-rich soils can have a large fraction of water that is bound to solid surfaces. The dielectric permittivity of bound water is lower than that of free water and can be temperature dependent (Or and Wraith, 1999). As a result, clay-rich soils may require soil-specific calibration and temperature corrections.

Point-scale measurements of water content can be made by using capacitance probes, time domain reflectometry (TDR), or time domain transmission (TDT) methods. Capacitance methods compare the capacitance of a circuit including a sample of soil to the capacitance of the circuit without the soil present to determine the relative apparent dielectric permittivity. TDR and TDT methods measure the velocity of propagation of a fast rise time electromagnetic signal through the medium along waveguides of known length to infer the relative apparent dielectric permittivity. Capacitance and TDR probes are used widely in hydrology and related fields because they allow for rapid, automated monitoring of water content within a small sample volume. In addition, TDR probes can be multiplexed readily and the probes can be designed to fit specific monitoring needs. TDT probes are not used as widely due to the need to connect wires to each end of the probe, making installation more difficult. However, due to the small sample volumes (tens of cubic centimeters) of TDR and capacitance instruments, individual probes cannot be used to monitor changes in water storage throughout the unsaturated zone. Rather, many of these probes must be used together to define the volumetric water content profile through time. However, automated depth profiling requires that each TDR or capacitance probe be connected, individually, to an instrument or data logger. While both TDR and capacitance probes have been designed to measure through access tubes, in practice this greatly restricts the sample volume of the instruments to the region immediately adjacent to the access tube. As a result, both the depth of investigation and the spatial resolution of the water content profile achievable with capacitance, TDR and TDT probes are limited. The primary contribution of capacitance, TDR and TDT probes to recharge monitoring lies in ability to collect their high temporal resolution data at single depths for calibration of unsaturated flow models. The case study, "Monitoring temporal changes in water storage with time domain reflectometry," provides an example where the high time resolution and ability to make automated measurements made TDR the ideal choice for recharge monitoring beneath an ephemeral stream. Robinson and others (2003) provide an extensive review of TDR.

Unlike TDR and TDT methods, ground-penetrating radar (GPR) instruments measure the velocity of propagation of unguided electromagnetic waves. Separate transmitting and receiving antennae generate and detect the electromagnetic (EM) energy. Antennae can be deployed either on or above the ground surface or in parallel boreholes. Surface applications typically produce radargrams, which show the strength of the received signal as a function of time since the source signal was produced. Analysis follows that developed for seismic methods, leading to images of subsurface reflectors that are associated with locations of sharp dielectric permittivity contrasts. Because GPR uses higher frequency sources than seismic methods, GPR offers greater spatial resolution than seismic methods; however, the maximum depth of penetration is much smaller. For example, while surface-based GPR can penetrate many tens of meters through ice, it may be limited to the shallowest several meters in clay-rich soils. Surface GPR methods are well suited to characterizing geologic structure in relatively shallow unsaturated zones. However, the method currently lacks sufficient spatial resolution and sensitivity to quantify changes in water content throughout the unsaturated zone to constrain unsaturated flow models. The spatial resolution of GPR may improve with advances in equipment and signal processing, but there is an inherent limitation of the depth of investigation of any surface-based method. In contrast, borehole GPR (BGPR) has been shown to be able to resolve the water content profile with very high spatial resolution to great depths. The ability of BGPR to characterize the water content profile rapidly and to great depths will likely lead to expanded use of the method for monitoring changes in water storage and for calibrating unsaturated flow models. An example of quantitative monitoring with BGPR is given in the case study "Monitoring infiltration and redistribution with borehole ground-penetrating radar." The primary limitation on the use of BGPR is the need for two parallel boreholes for each measurement location. The cost of borehole installation will likely relegate this method to limited application in areas of particular interest within a basin. Huisman and others (2003) provide an excellent review of GPR.

Electrical Conductivity

The electrical conductivity describes the ability of a medium to transmit electric current in accordance with Ohm's law applied to a multiphase porous medium. In general, the bulk electrical conductivity of a medium depends

Monitoring Temporal Changes in Water Storage with Time Domain Reflectometry

By Kyle W. Blasch

A two-dimensional array of time-domain reflectometry (TDR) probes was installed perpendicular to the path of streamflow in a 60-m wide, coarse-grained alluvial channel. The study site was located where Dodge Boulevard crosses Rillito Creek, about 3 km west of Swan Road (fig. 1). The array was used to measure changes in soil water content at the onset and cessation of ephemeral streamflow events. The changes in the water-content profiles with time were used to quantify infiltration at the onset of streamflow and redistribution at the cessation of streamflow. In addition, the data were used to infer the timing of onset and cessation of streamflow. TDR was selected because it provides rapid, automated measurements of water content with little need for medium-specific calibration. For this study, it was also critical that the TDR probes could be installed in the streambed beneath the zone of scour.

The volumetric water content was measured at 2-minute intervals from July 2000 through December 2002 using 28 TDR probes installed in a trench, arranged in four vertical profiles, spaced 3 m apart (fig. 3). Twenty-eight type-T thermocouple probes were collocated with the TDR probes. The southernmost instrument profile was installed at the point of lowest elevation in the channel cross section, approximately 4 m from the south bank. TDR probes were placed at depths of approximately 0.50, 0.75, 1.0, 1.25, 1.50, 2.0, and 2.5 m below the stream channel surface. A Campbell Scientific TDR100 time domain reflectometer was used in conjunction with a Campbell Scientific CR10X data logger to transmit, receive, and convert waveforms into volumetric water content. TDR probes were constructed from two stainless steel wave-guides 0.20 m in length, spaced 0.03 m apart. Probes were connected by coaxial cable (RG-8; 50-ohm impedance, 2.6-millimeter diameter center conductor) to minimize signal attenuation between the probes and the TDR100 instrument. Cable lengths ranged from 11 to 26 m. Each probe was calibrated in the laboratory with the RG-8 cable attached. The precision of the water-content measurements was approximately 0.03 cubic meter of water per cubic meter of bulk sediment (m^3/m^3). Copper-constantan thermocouple probes were operated using a Campbell Scientific CR10X. Temperature sensors were programmed to measure temperature every 5 seconds and to record a time-averaged temperature at 5-minute intervals with a precision of 0.1°C.

The water content generally increased from about 0.20 to 0.35–0.40 m^3/m^3 within 10 minutes of the onset of streamflow (fig. 4). Vertical infiltration rates were estimated from the velocity of the wetting front and from the measured water contents. The wetting front velocity was determined by dividing the depth of the deepest probe minus

Figure 3. Photograph and schematic of two-dimensional array of sensors within the Rillito Creek stream-channel deposits, Tucson, Ariz.

0.5 m by the elapsed time between an increase in water content exceeding 0.05 m^3/m^3 at 0.5 m and an increase in water content to more than 0.30 m^3/m^3 at the deepest probe. The infiltration flux at the onset of flow was as high as 300 m/d, with higher infiltration rates associated with lower antecedent water contents, which agrees with the values reported in a previous investigation in Rillito Creek (Wilson, 1980). The infiltration rate reduced by an order of magnitude within minutes and continued to decrease as water percolated to greater depths. Late-time redistribution occurred at a rate of approximately 0.12 m/d, which is lower than the reported range of 0.34 to 1.1 m/d for steady state infiltration flux reported previously for this site (Turner, 1943; Katz, 1987).

Vertical redistribution fluxes at the cessation of streamflow averaged about 0.12 m/d. Variability among redistribution fluxes shows strong correlation with temperature, with the magnitude of the redistribution flux increasing with increasing temperatures. Specifically, redistribution fluxes ranged from about 0.07 m/d for sediment and fluid temperatures near 10°C to 0.17 m/d for temperatures near 30°C. Water content measurements were used in conjunction with temperature and pressure measurements to constrain a variably saturated heat and fluid flow model of the upper 2.5 meters of the subsurface. This model was used to infer hydraulic properties of the soil (Blasch, 2003).

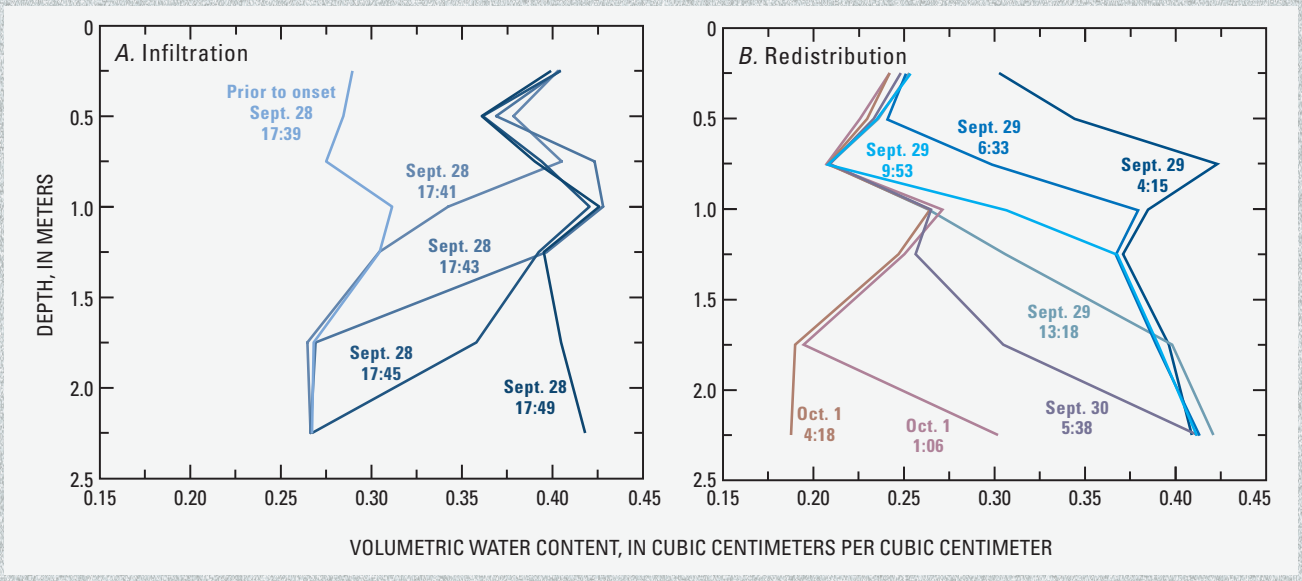

Figure 4. Change in volumetric water content of the stream-channel deposits at: *A*, The onset of an ephemeral event on September 28, 2000; and *B*, The cessation of the ephemeral event.

Monitoring Infiltration and Redistribution with Borehole Ground-Penetrating Radar

By Andrew M. Binley

Borehole ground-penetrating radar shows promise for investigating focused ground-water recharge in arid and semi-arid environments. This sidebar illustrates its potential by summarizing results of borehole ground penetrating radar (BGPR) surveys conducted at a field site in the United Kingdom.

The Permo-Triassic Sherwood Sandstone is a major groundwater resource subject to increasing demand for public and private water supply. The aquifer is threatened by heavy chemical loading from agricultural practices. Consequently, models are required in order to assess travel times and attenuation within the unsaturated zone. Recent work demonstrated the value of borehole geophysical methods for monitoring water flow through the unsaturated zone (induced by natural and tracer loading) at two sites (Binley and others, 2001; Binley, Cassiani, and others, 2002, Binley, Winship, and others, 2002). Results for one of the sites are shown here.

The site, near Hatfield, South Yorkshire at the Lings Farm smallholding (National Grid Reference SE 653 079), was instrumented during June and July of 1998. The site is an example of potentially vulnerable sandstone islands, a term used by UK environmental regulators to indicate areas of relatively clay-free drift deposits that allow direct and rapid recharge to the underlying sandstone aquifer relative to clay-covered areas. Because such areas permit potentially rapid, poorly attenuated, contaminant transport to the water table, the hydrological characterization is essential for accurate vulnerability evaluation.

Two boreholes (H-R1 and H-R2) were drilled 5 m apart at the site for deployment of borehole radar. Two 102-millimeter (mm) diameter cores (H-M and H-AC) were drilled near to H-R1 and H-R2 by Leeds University, UK. Drift thickness at the site is typically 2–3 m and consists of mainly fluvio-glacial sand and gravel. From analysis of the cores, the sandstone sequence at the site consists of fluvially derived fining upwards sequences 1–3 m thick, grading from medium grained to fine grained sandstone. Pokar and others (2001) present physical and hydraulic analysis of samples extracted from a core at the site. Two main distinguishable lithologies are medium-grained sandstone, which comprises the bulk of the core, and fine and medium sandstone, subhorizontally laminated on a millimeter scale.

Specimens from the core were extracted by Leeds University for measurement of the dielectric permittivity under varying volumetric water contents. West and others (2003) show that for 100 MHz frequency measurements a value of relative permittivity $\kappa = 5$ is appropriate for the main lithological unit of the core.

To determine dielectric properties at the field scale, borehole-to-borehole surveys may be conducted in two transmission modes. In both cases, a radar signal is generated from a transmitter placed in one borehole with a receiver deployed in the other. Measurement of the travel time of the received wave permits determination of the first arrival and, hence, the apparent velocity of the electromagnetic wave. In one mode, using a multiple offset gather (MOG), the receiver is moved to different locations in one borehole whilst the transmitter remains fixed. The transmitter is then moved and the process repeated. Following collection of all data in this mode and determination of the travel time for each wave path-line it is possible to derive a tomogram of velocity within the plane of the borehole pair. In contrast, a zero offset profile (ZOP) may be determined by placing the transmitter and receiver common depths for each measurement. By systematically lowering or raising the pair of antennae in the two boreholes, it is possible to obtain a one-dimensional profile of travel time over the entire borehole length. Typically, MOG surveys offer two-dimensional discrimination of the water content or change in water content at the expense of greater measurement times.

Borehole-to-borehole radar measurements in ZOP mode were conducted at the Hatfield site between February 1, 1999, and November 19, 2000, at approximately monthly intervals. During 1999, a number of MOG surveys were also carried out at the site. For all surveys, the Sensors and Software (Mississauga, ON, Canada) PulseEKKO borehole radar system was used with 100 MHz borehole antennae. Surveys were conducted using 0.25-m depth intervals between antennae positions over the range 1–12 m below ground level. Typical survey times were 2 hours for MOG mode and 5 minutes for ZOP mode. Instrument calibration was carried out

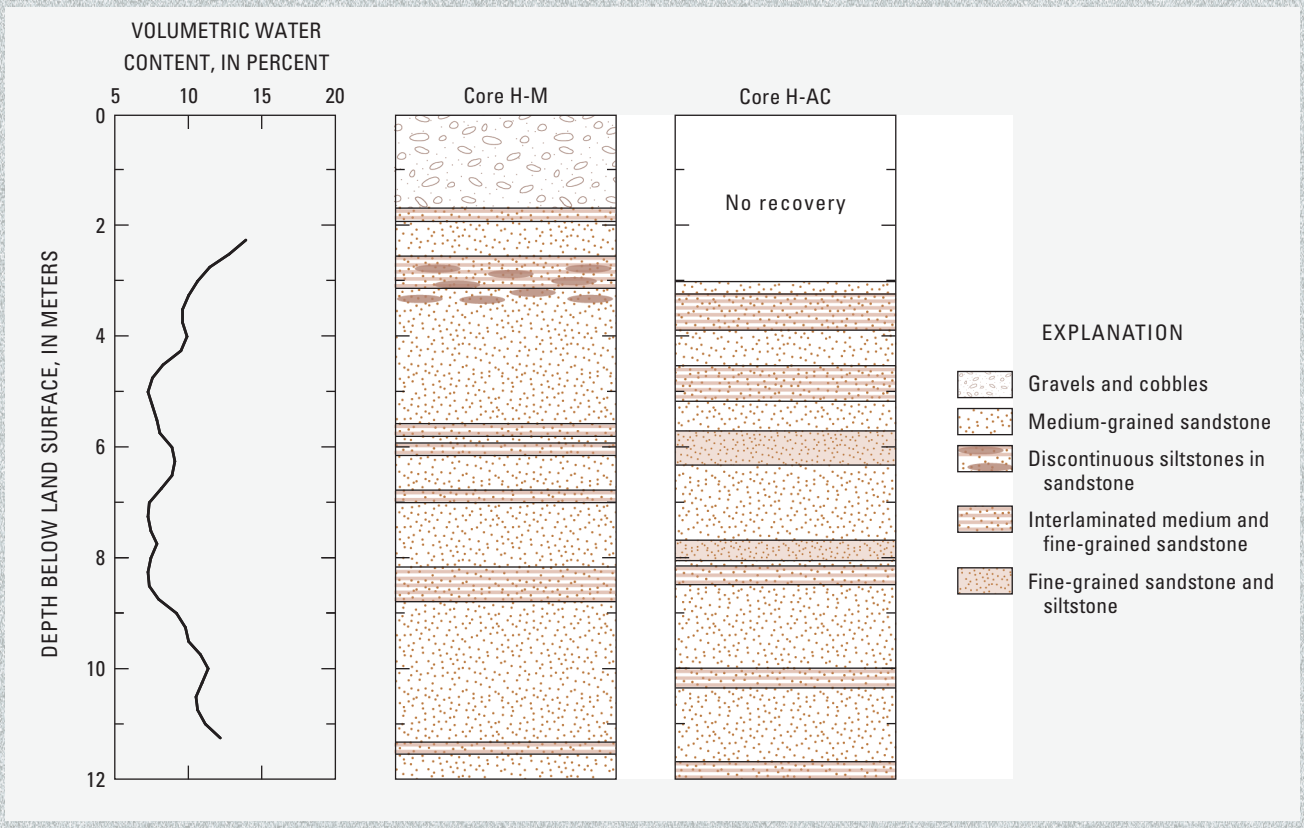

Figure 5. Radar derived volumetric water contents on February 1, 1999, at the Hatfield site together with core lithologic logs.

prior to and following each mode of survey and regularly during each MOG survey to remove instrument drift. For both survey modes first time arrivals were picked manually. Tomographic analysis of the MOG data was carried out by using the straight-ray inversion procedure of Jackson and Tweeton (1994) using a discretization of 0.5 m in the horizontal and 0.25 m in the vertical. A repeat set of measurements was made for each ZOP survey. The average, manually picked, first arrival travel time from the two measurements at each depth was used to define the volumetric water content profile with depth.

The volumetric water content profile was collected on February 1, 1999, at the Hatfield site with a ZOP BGPR survey (fig. 5). The volumetric water content varied from 0.6 to 0.16 m^3/m^3 and showed some correlation with the lithologic information provided by the core logs (J. West, oral commun., 1999). A comparison of the core logs illustrates that the tops of the fine-grained units are not necessarily horizontal because these are erosional contacts (fig. 5). The logs do show, however, similar larger scale characteristics, see for example the fine-grained units at approximately 6-, 8- and 10-m depths. The layers at 6 and 10-m depth are also associated with zones of higher volumetric water content.

Seasonal characteristics of precipitation at the Hatfield site are the occurrence of main net inputs during September to January with a number of spring events during March or April, followed by relatively high evapotranspiration during summer. The monthly net rainfall estimates at the Hatfield site for the period July 1, 1998, to December 31, 2000, and the temporal dynamics of water content change throughout the profile are compared in figure 6. The shape of the response in the upper sandstone follows the seasonal pattern of the net rainfall. Note the reduction in

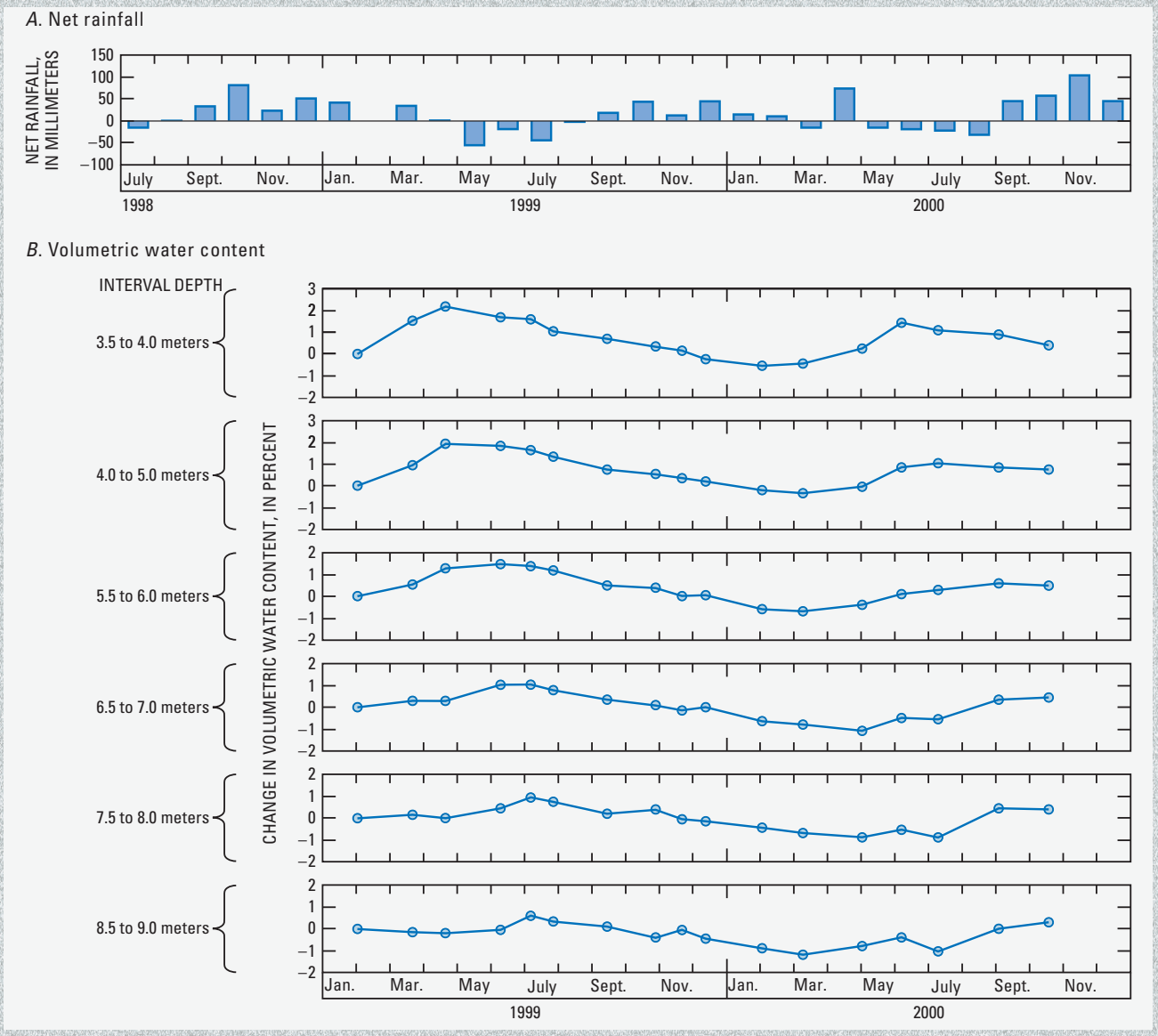

Figure 6. *A*, Net rainfall series, and; *B*, Change in volumetric water content over selected depth intervals using zero offset profile (ZOP) radar estimates, Hatfield site. All differences are relative to February 1, 1999.

volumetric water content changes for the peak in 2000 in comparison to the peak in 1999 because of significantly reduced rainfall during winter 1999. The delays in wetting and drying patterns are also clearly visible over this interval when compared with the rainfall input series, as is the smooth cyclic pattern, both demonstrating the impact of drift cover. More significant, however, is the transmission of this signal throughout the profile. A delay of two to three months in the initial peak is apparent when comparing series at 3.5 to 4 m and 6.5 to 7 m. A similar delay is also apparent in the propagation of the drying front. It is interesting to note the marked change in the time series for the 5.5 to 6 m and 6.5 to 7 m intervals, indicating that the transmission of the wetting front appears geologically controlled at about 6 m. This may be due to the low permeability unit identified on the core logs (fig. 5). This is also consistent with the observed response during tracer experiments at the site (Binley and others, 2001).

The change in volumetric water content determined from selected MOG surveys reveals a more complex evolution of wetting and drying fronts within the sandstone (fig. 7). The impact of the high net rainfall during March 1999 can be seen clearly at a region of high positive water storage change that advances to a maximum depth of 7 m by June 1999. Through the summer of 1999 emergence of a drying front can be seen which continues to develop through to winter 1999. The tomograms also show the effect of the impeding layer previously referred to between 6 and 7 m depth, during the drainage period.

The examples shown here demonstrate the potential value of BGPR for monitoring recharge processes. Our results indicate that, at least for the sandstone site reported here, we are able to resolve changes of less than one percent absolute moisture content. The method allows greater assessment of spatial variability of recharge dynamics than conventional localized measurement approaches (TDR, neutron probe, and so on). When used in profile (ZOP) mode, the method permits an integrated measure of changes in moisture content between two boreholes and, as such, uses a measurement support volume potentially more appropriate for modeling unsaturated zone processes.

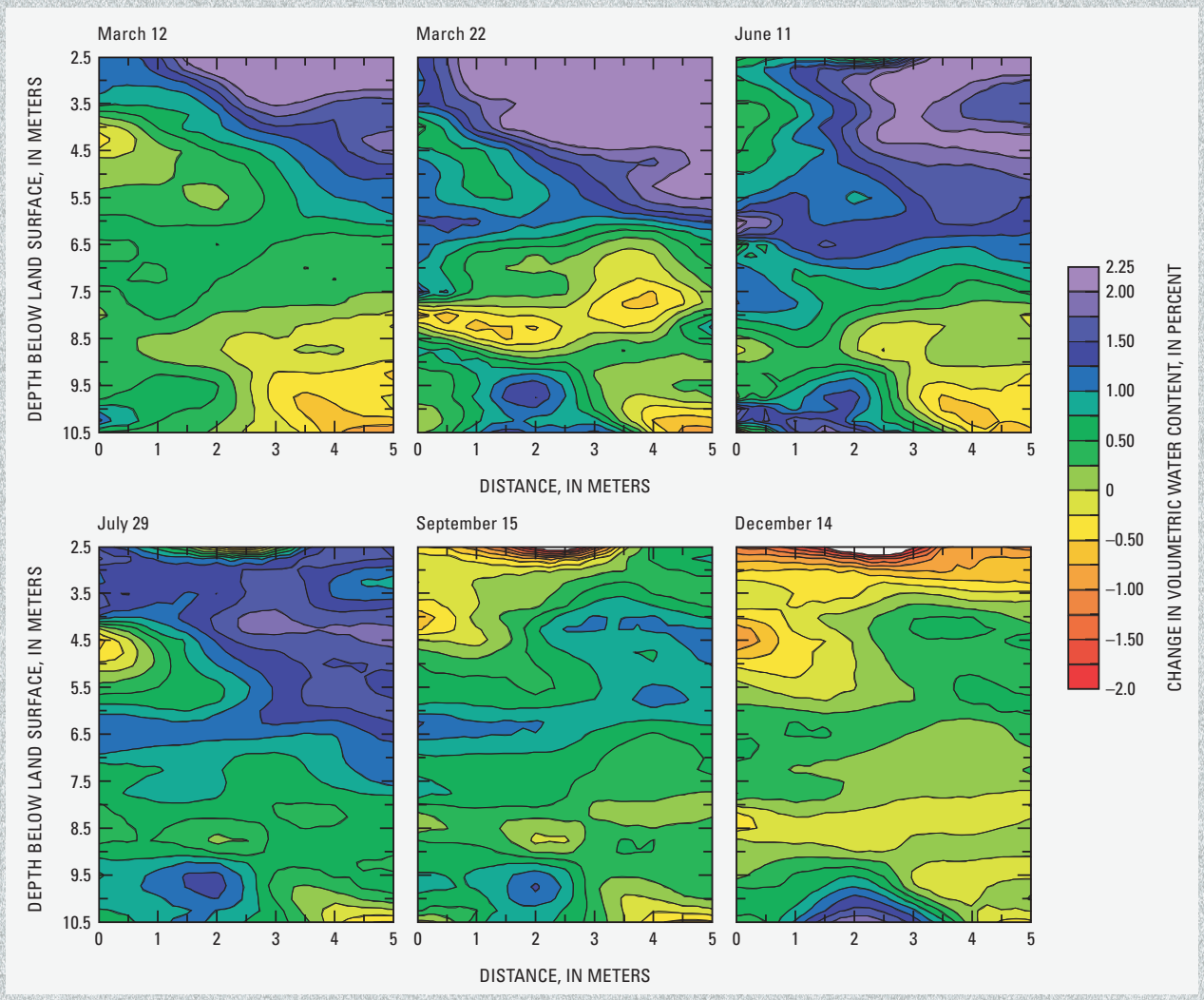

Figure 7. Change in volumetric water content using multiple offset gather (MOG) borehole ground penetrating radar (BGPR) surveys. All differences are relative to February 1, 1999.

on the electrical conductivities of the constituents of the medium. This dependence is described as

$$\sigma_b = \sigma_w \varphi^m S^n + \sigma_s \ , \qquad (2)$$

where

σ_b = the bulk electrical conductivity (1/ohm-L),

σ_w = the pore water electrical conductivity (1/ohm-L),

φ = the porosity (volume of pores per bulk volume),

S = the water saturation (volume of water per volume of pores), and

m, n = empirical fitting parameters (Archie, 1942).

The final term, σ_s (1/ohm-L), has been added to describe the contribution of the electrical conductivity of the soil solids to the bulk electrical conductivity (for example, Patnode and Wyllie, 1950; Waxman and Smits, 1968). The dependence of the bulk electrical conductivity on several properties limits the uniqueness of the interpretation of any one property (water content, for example) from the measured bulk electrical conductivity. However, for many recharge studies, the water quality does not vary enough with time or space to give rise to changes in the pore water electrical conductivity that are large enough to affect interpretations of the water content distribution. In the absence of clay-rich soils, the porosity and the electrical conductivity of the soil solids are nearly constant throughout the unsaturated zone, as well. In most cases, the porosity and electrical conductivity of the soil solids are constant in time. This offers the possibility of location-specific calibration or the use of measured bulk electrical conductivity changes to infer temporal changes in the water content distribution.

The electromagnetic geophysical methods that currently show the most promise for application to recharge monitoring are time domain reflectometry (TDR), time domain transmission (TDT), ground penetrating radar (GPR), capacitance probes, electrical resistance probes, electrical resistance tomography (ERT), electromagnetic induction (EMI), time domain electromagnetics (TEM), self potential or streaming potential (SP), controlled source audio magnetotellurics (CSAMT), and nuclear magnetic resonance (NMR). TDR, TDR, capacitance probes, and GPR are used primarily to measure dielectric permittivity, as discussed above. ERT, EMI, TEM, and CSAMT are used primarily to measure the electrical conductivity distribution of the subsurface. These methods can be divided into direct and inductive methods on the basis of how electrical energy is applied to the ground and how the electrical response of the subsurface is measured. Directly coupled methods require that electrodes be inserted into the ground to apply electrical current and to measure voltage. Inductively coupled methods typically use coils to apply electrical current and to measure voltage, thereby eliminating the need to insert electrodes into the ground. (CSAMT is a hybrid method in which a directly coupled source and both directly and inductively coupled receivers are used.) Electromagnetic methods for measuring the electrical conductivity distribution can be separated further into time domain methods, which measure the electrical conductivity over many frequencies simultaneously, and frequency domain methods, which measure over singles frequencies. TEM is an example of a time domain method, while ERT, EMI, and CSAMT are frequency domain methods. Telford and others (1990) and Rubin and Hubbard (2005) provide reviews of electromagnetic methods.

The design of direct current (or low frequency) EM methods allows for great flexibility in sampled volume, measurement sensitivity, and distribution of measurement sensitivity within the sampled volume. Typically, each measurement is made with four electrodes. Two electrodes are inserted into the ground and used to inject current. The remaining two electrodes are inserted into the ground and used to measure an electrical potential. SP methods are an intriguing variation of direct current electrical conductivity methods in which current is generated naturally due to the flow of water in the subsurface. This method offers the ability to identify regions in the subsurface through which water is flowing. With further development, SP methods combined with other methods may be able to quantify water flux. ER and SP methods use similar instruments and survey designs, so they will be discussed together. The size of the sample volume and the measurement sensitivity within the sample volume of these instruments are controlled by the separations of the electrodes; generally, larger separations lead to larger sample volumes. Further refinement of the sensitivity distribution can be achieved by the choice of array type (the relative positions of the four electrodes). Point scale measurements of the bulk electrical conductivity can be made by using closely spaced electrodes either at the ground surface or within boreholes. The simultaneous inversion of multiple measurements made at the ground surface, in boreholes, or some combination of both, leads to a two- or three-dimensional image of the subsurface bulk electrical conductivity distribution. This is known as electrical resistance tomography (ERT). Modern advances in ERT instrumentation allow for automated selection of electrode sets to conduct many measurements with different combinations of stationary electrodes. This ability makes ERT particularly useful both for structural mapping and for time-lapse monitoring. Because of the sensitivity of the bulk electrical conductivity to properties of both the medium (porosity, solid electrical conductivity) and the fluid (water saturation, pore water electrical conductivity), ERT is less useful for stand-alone structural mapping than seismic methods. However, when used in conjunction with other methods (seismics, for example), ERT can improve structural mapping and can be used for water content mapping and monitoring. Based on these qualities of ERT, together with the ability of ERT to construct multidimensional images from static instruments, it is likely that ERT will be applied more routinely for monitoring changes in water

content throughout the unsaturated zone both for constraining detailed hydrologic models and for direct interpretation of the water fluxes during transient infiltration. ERT has been applied widely in hydrologic studies and many examples of its successful use have been published. The great flexibility of the ERT method to allow for novel applications is demonstrated through the steel-casing resistivity technology (SCRT) variation of the mise-a-la-masse method described by Telford and others (1990, p. 523) in the case study "Temporal monitoring of infiltration by using a hybrid electrical method."

As with the directly coupled low frequency EM methods, there is also a wide variety of designs of inductively coupled electrical conductivity measurement devices. Typically, these instruments are comprised of two coils. One coil applies a time-varying EM field. The second coil measures secondary currents that are induced in conductive bodies in the subsurface. Frequency domain methods measure the applied and induced signals simultaneously while the signal is applied; the induced field is determined by nulling or accounting for the primary field. Time-domain methods measure the time rate of decay of the induced currents after the source current has been turned off. The size of the sample volume and the measurement sensitivity within the sample volume are controlled by the separation of the coils and the frequency of the applied signal. Generally, larger separations and lower frequencies lead to larger sample volumes and lower resolution within the sample volume. Inductively coupled EM methods range from very small scale (hand held metal detectors and down-hole EM tools, for example) to very large scale (TEM, for example) with an instrument available for almost every intermediate scale of measurement. EM induction methods can also be used to profile through a nonmetallic borehole, providing very high resolution of the electrical conductivity profile. Callegary and others (2007) analyze spatial resolution and exploration depth of low-induction-number frequency-domain electromagnetic induction methods.

Inductive EM techniques are most likely to contribute to recharge monitoring either through definition of geologic structure (especially airborne methods and borehole logging) and through time-lapse monitoring at smaller scales or at single locations. Two examples are provided to demonstrate the use of frequency domain methods. "Use of electromagnetic logs to monitor downward movement of focused infiltration" describes the quantitative use of borehole EM for monitoring infiltration. Depth profiling with surface-based frequency domain methods requires the use of different frequencies and different coil separations, limiting the practically achievable temporal and spatial resolution of the electrical conductivity profile. Time domain methods measure over a wide range of frequencies in a short time, allowing for efficient depth profiling. However, because these methods typically require the use of relatively large antennae loops, they are difficult to deploy quickly at many surface locations, limiting spatial coverage. The ability of time domain electromagnetic methods to make rapid, nondestructive measurements of electrical conductivity suggests that these methods could contribute to monitoring transient infiltration and to calibrating numerical models describing water flow throughout the unsaturated zone. However, quantitative application of these methods for recharge monitoring will require improved understanding of the spatial resolution of TEM methods to subsurface water content distributions. Therefore, borehole logging remains the most useful approach to depth profiling for hydrologic investigations. "Electromagnetic induction as a reconnaissance tool to map recharge" examines the use of surface-based EM to map likely areas of recharge. This case study is of particular interest because EM mapping is often included in hydrogeologic investigations because the lack of direct contact of the instrument with the ground allows for rapid mapping of lateral changes in hydrogeologic structure over large areas.

Proton Precession

Protons of hydrogen atoms in water molecules have a magnetic moment that aligns with an external magnetic field. Typically, this magnetic moment is aligned with the local magnetic field of the earth. When another magnetic field is applied, the axes of the spinning protons are deflected to align with the total field. When the applied field is removed, the protons realign with the local magnetic field of the earth. As the protons realign, they generate a relaxation magnetic field. Nuclear magnetic resonance (NMR) methods measure this relaxation magnetic field in response to a magnetic field due to an alternating current in a loop placed on the ground surface. The instrument response is a time-varying, time-decaying voltage measured with either the same loop or a secondary loop. The initial amplitude and rate of decay of the measured voltage is related to the volumetric water content of the subsurface. The water-content profile can be inferred based on measurements made with a range of excitation intensities. In addition, the decay time can be related to the mean pore size, giving an indication of the hydraulic conductivity (Yaramanci and others, 1999). As with most surface-based geophysical methods, the resolution and accuracy of the method decrease with depth. Currently, 100–150 m depth can be investigated with a resolution of a few decimeters at shallow depths and a few meters at greater depths. The accuracy achievable for water content is roughly a few percent, depending on depth. NMR is a promising new method for rapid profiling to great depths, but the method is currently in too early a stage of development to present a case study for recharge monitoring.

Mass Change

The gravitational attraction at a point on the surface of the Earth depends primarily on the density distribution of the materials in the subsurface. Gravity methods have long made use of spatial changes in the subsurface density distribution to define geologic structure. However, given that water is less dense that geologic materials and that the shape of the water table typically changes gradually with lateral distance (unless

Temporal Monitoring of Focused Infiltration using a Hybrid Electrical Method

By James B. Fink and Marc T. Levitt

A performance evaluation test was performed at the Hanford Nuclear Reservation in Benton County, eastern Washington State to meet U.S. Environmental Protection Agency and American Society of Testing and Materials protocols for statistically determining the effectiveness of electrical geophysical methods for monitoring leaking underground storage tanks using measurements made exclusively exterior to the tank. Although the controlled leak sources were released at points, the results can be extended to electrical geophysical methods for monitoring infiltration beneath planar sources, such as recharge impoundments, ephemeral streambeds, or basin floors under field conditions. The location of the test at the Hanford facility was of particular interest for recharge investigations because of its thick unsaturated zone and desert conditions, making it a useful model for much of the western U.S. As part of this investigation, a new application, called steel casing resistivity technology (SCRT), was evaluated.

The target of the investigation was a mock-tank cold test facility in the 200 East area of Hanford (NRC, 2001). The mock tank is a two-thirds-scale mock-up of a million-gallon (3,800 cubic meters), single-shell-tank (SST) such as those buried in several tank farms at Hanford. The 15-m diameter mock-tank was partially buried to better simulate tank-farm conditions with the bottom of the tank 1.2 m below ground surface and the top of the tank 3.0 m above the ground surface. Figure 8 shows a plan view of the mock tank and related infrastructure. Fourteen injection points were in the base of the mock-tank to simulate point-source leaks beneath SSTs.

The mock tank is placed in the Hanford formation, a permeable, unconsolidated sand and gravel sequence ranging in thickness from 60 to 100 m. The formation is characterized by little or no clast cementation and few fine-grained horizons. Gravel content is commonly more than 40 percent. Depth to water beneath the mock tank is approximately 60 m. The Hanford formation typically has a volumetric water content of 0.06 m^3/m^3. The saturated volumetric water content ranges from 0.12 to 0.38 m^3/m^3. The saturated hydraulic conductivity ranges from 4×10^{-6} to 2×10^{-4} m/s.

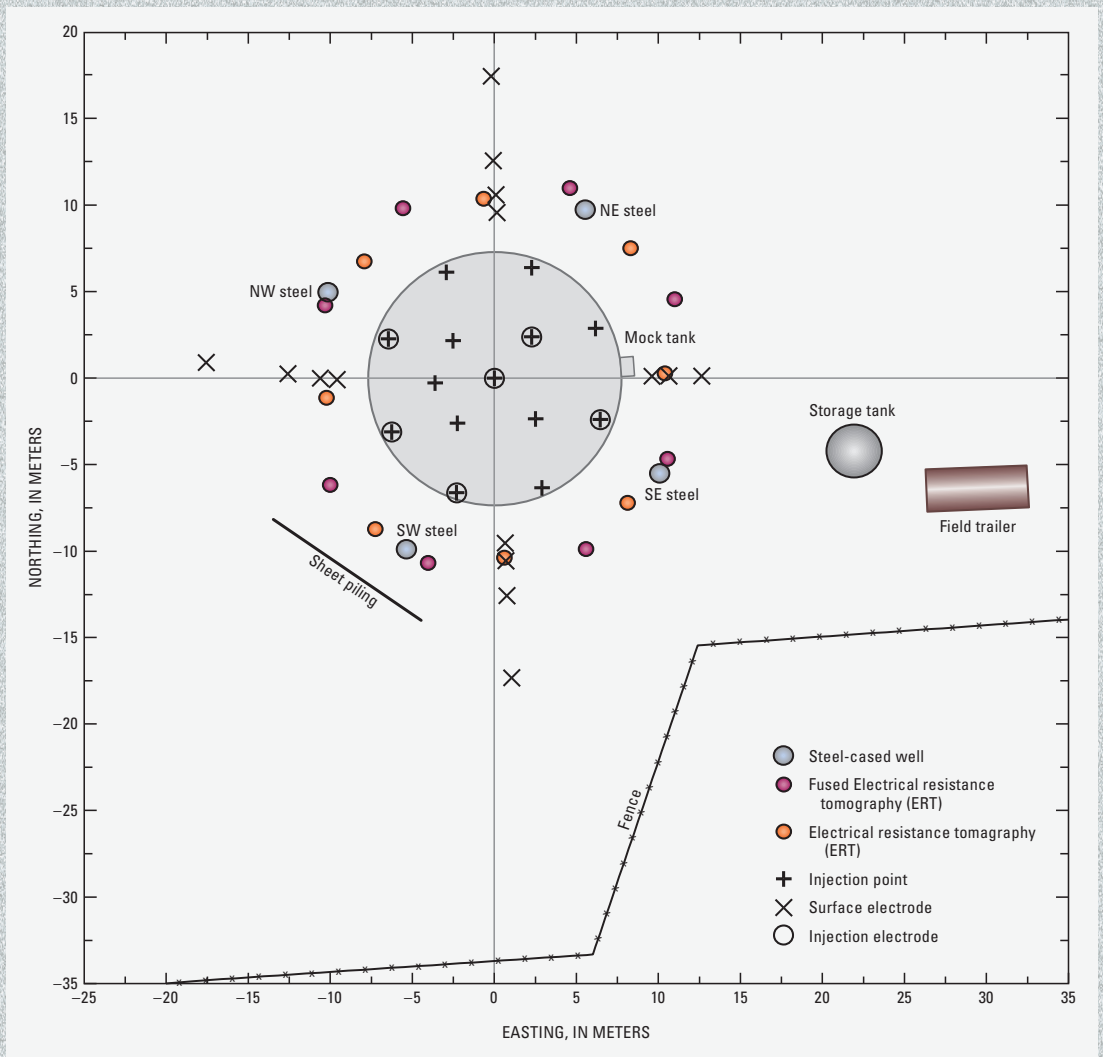

Figure 8. Plan view of the mock tank and test-related infrastructure at the Hanford site.

Generally, the Hanford formation allows rapid vertical infiltration. The Hanford formation is underlain by a Pliocene–Pleistocene unit, which constitutes an impermeable clay-and-caliche-rich zone up to 8-m thick and variably present throughout the facility. This confining unit is either absent beneath the mock tank facility or sufficiently deep to have no effect on infiltration within the depth of this investigation.

The solution used for the test was 36 percent by weight sodium thiosulfate pentahydrate ($Na_2S_2O_3$–$5H_2O$). This solution was selected to simulate the specific gravity, concentration, relative viscosity, and electrical conductivity of typical tank waste. A total volume of about 51 cubic meters (m^3) was released in 14 leak events of approximately 4.6 m^3 each. Test leak rates were 0 (no-leak), 7.6, 38, and 76 liters per hour (2, 10, and 20 gallons per hour). Specific leak timing was unknown to monitoring personnel.

Sixteen vertical electrode arrays had been placed uniformly around the mock tank by direct push technology. Each array was located approximately three meters away from the edge of the mock tank. Each array was made up of eight stainless steel screen electrodes approximately ten centimeters long and spaced equally from a few centimeters to ten meters below surface. In addition to the point electrode arrays, four steel casings were installed to simulate drywells surrounding the tanks within the tank farms. One casing was placed in each quadrant around the tank. Each casing was about three meters from the tank and extended to a depth of about ten meters. A steel sheet piling about five meters tall by ten meters wide was placed to the southwest of the mock tank to represent the effects of an adjacent tank. The sheet piling was electrically connected to the mock tank for the majority of the testing period. It was disconnected as an additional complicating factor during a brief portion of the test.

The SCRT measurements were collected continuously throughout the 110-day test except for a two-hour period each day when ERT data were acquired. Each SCRT sweep required approximately 15 minutes. Approximately 3.8 million data points were acquired during the test. The SCRT surveys made use of the four steel dry-well casings and the eight electrically shorted ERT arrays that were intended to approximate drywell casings. In addition, the steel mock tank, the injected solution, surface electrodes and other electrically grounded infrastructure were used to inject current and to detect potential distributions. This use of the tank and the leaked solution is an important difference between conventional ERT methods and the SCRT approach. This direct connection to the leaking solution allowed SCRT to acquire mise-a-la-masse type data by energizing the leaking solution. The reciprocal arrangement of receiving on the tank while energizing a dry well, for example, performed equally well. All data acquisition activities were controlled remotely through a virtual private network that was accessible via the Internet. All instruments were kept in a climate-controlled, temporary enclosure on-site at the mock tank and powered from the regional electrical grid.

The SCRT results include measurements with many combinations of electrodes and electrode types. For ease of visualization, the SCRT time series for one dry-well sensor is shown in figure 9 for a portion of the test. The abscissa is time in decimal days. The ordinate of the SCRT time series is normalized transfer resistance; that is, the normalized intensity of the electric field measured using a four-electrode array. The leak events are indicated by increasing portions of the cumulative infiltration-volume curve. The leaks and intervening non-leak periods are readily seen as sudden changes in the SCRT time series at both the onset and the cessation of each leak. Such well-defined offsets in the time series could offer accurate, long-term, quantitative monitoring of the timing of leak activity. After compensation for cultural distortions of the local electric field, the change in transfer resistance with time during leak periods is highly correlated with the leak rate. The time series collected at other locations show similar patterns through time, but different amplitudes reflecting the length of the electrode, distance from the leak, and location within the background electric field. Such techniques provide possibilities for long-term, semi-automated monitoring of ground-water recharge from ephemeral stream infiltration.

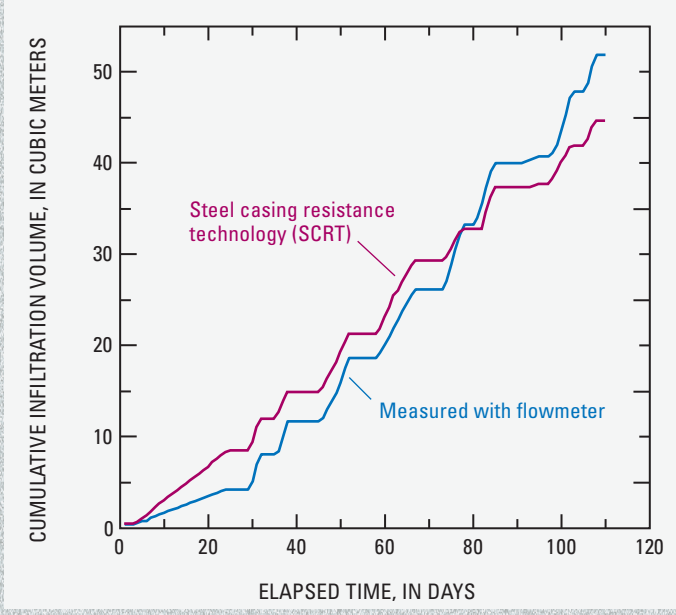

Figure 9. Measured and steel casing resistance technology (SCRT) derived infiltration volume during the entire leak test.

Use of Electromagnetic Logs to Monitor Downward Movement of Focused Infiltration

By John A. Izbicki and Steven M. Crawford

An experiment was conducted to determine if water infiltrated from a 0.4-hectare artificial recharge pond could recharge the water table about 122 m below land surface. The facility was located along Oro Grande Wash in the western Mojave Desert, near Victorville, Calif. (fig. 10). About 580,000 m^3 of water was infiltrated during three periods from October 1 to December 19, 2002; February 10 to March 24, 2003; and May 10 to September 31, 2003. The pond was allowed to dry between infiltration periods and accumulated fines were removed before more water was infiltrated.

The downward movement of water in the unsaturated zone beneath the pond was monitored at an instrumented borehole adjacent to the pond by using a variety of techniques. The U.S. Geological Survey installed the borehole in January 2001. Air, rather than water, was used to drill the borehole and remove drill cuttings. Steel casing stabilized the borehole during drilling and instrument installation. The cuttings from the hole were logged at 0.3-m intervals. On the basis of those logs, the 0.22-m diameter borehole was instrumented with three tensiometers connected to land surface with 0.025-m diameter PVC pipe, eight heat-dissipation probes, five suction-cup lysimeters, and a 0.05-m diameter PVC well screened across the water table. The well also served as an access tube for repeated logging with geophysical tools. Each instrument was packed in suitable material to allow communication with the formation (combinations of 60-mesh sand and diatomaceous earth) and isolated vertically with low-permeability bentonite grout to prevent flow of water within the borehole during the experiment. The grout was installed dry, and hydrated in the borehole within several weeks of installation. The steel casing used to stabilize the borehole was removed as the instruments and backfill material were installed.

The tensiometers and heat-dissipation probes installed within the borehole recorded changes in matric potential at 4-hour intervals during the recharge experiment. The tensiometers recorded both matric potential and head (positive pressures). In addition to changes in moisture content, the tensiometers also were sensitive to changes in air pressure and compression of the unsaturated material beneath the pond from the weight of the infiltrated water. The heat-dissipation probes measured only matric potential and were not sensitive to changes in air pressure or compressional forces. Both the tensiometers and heat-dissipation probes responded to the rapid downward movement of a small amount of water in advance of the main wetting front.

The position of the wetting front also was measured intermittently during the experiment with an electromagnetic induction (EMI) geophysical tool. In this case, an EMI tool was chosen rather than a neutron probe because of the likelihood that the hydrated bentonite grout used to seal the borehole would lead to an unacceptably small sensitivity of the neutron probe to the surrounding medium. The EMI tool has a larger sample volume, making it sensitive to changes in the moisture content of the native material beyond the grout.

Selected EMI logs collected between November 11, 2002, and May 6, 2003, show the downward movement of water in the upper 75 m of the borehole (the lower 47 m are not shown; fig. 11). Increased water content as the wetting front progressed downward was recorded as increased electrical conductivity on the EMI log. The downward rate of movement of the wetting front ranged from 0.75 to 0.06 m/d (fig. 12). The position of the wetting front measured with the EM logs and other instruments within the borehole show good agreement throughout the experiment. The downward rate of movement, initially as high as 1 m/d, decreased through time to a relatively constant rate of about 0.08 m/d (fig. 12). Assuming no impermeable units were encountered, the wetting front was estimated to reach the water table underlying the pond by late February 2005 (fig. 12). The downward rate of movement of the wetting front decreased rapidly at the beginning of the experiment as the wetting front spread laterally in the subsurface. The downward rate of movement of the wetting front decreased further between December 22, 2002, and May 6, 2003, when water was not being continuously infiltrated from the pond.

Decreased water content, recorded as decreased electrical conductivity on the EMI logs (fig. 11), also was measured at certain depths within the unsaturated zone during the recharge experiment. The largest decreases occurred after water accumulated on top of coarse-grained gravel layers. Saturated conditions developed on top of these layers until the pressure exceeded the entry pressure of the underlying coarser-grained deposits. Once the entry pressure was exceeded the water drained rapidly to greater depths. Smaller decreases in resistivity were associated with redistribution of previously infiltrated water to greater depths when no water was being infiltrated at the ground surface.

The arrival of the wetting front estimated from heat-dissipation probe data appears to lag the arrival estimated on the basis of tensiometer and EM log data (fig. 12). This probably results from the placement of the instruments within the borehole. For example, several heat-dissipation probes were placed beneath clay layers thought to impede the downward movement of water.

Borehole logging instruments allow more flexibility in a monitoring program than buried instruments. For example, in this study, the EM data could have been collected at any time to determine the position of the wetting front. This would

not possible be with the instruments that were installed at a fixed depth, which require that the depth of the wetting front be inferred between measurement points. The EM logs also yielded information throughout the entire thickness of the unsaturated zone and were sensitive to the dynamic movement of water within the subsurface in both fine-grained and coarse-grained units. The EM logs were not sensitive to confounding influences from air-pressure changes or compression of unsaturated material as the water from the pond moved downward. As a result, borehole EM data were useful for monitoring wetting front movement and for predicting the arrival of the infiltrated water at the water table, especially when used together with traditional unsaturated-zone monitoring techniques.

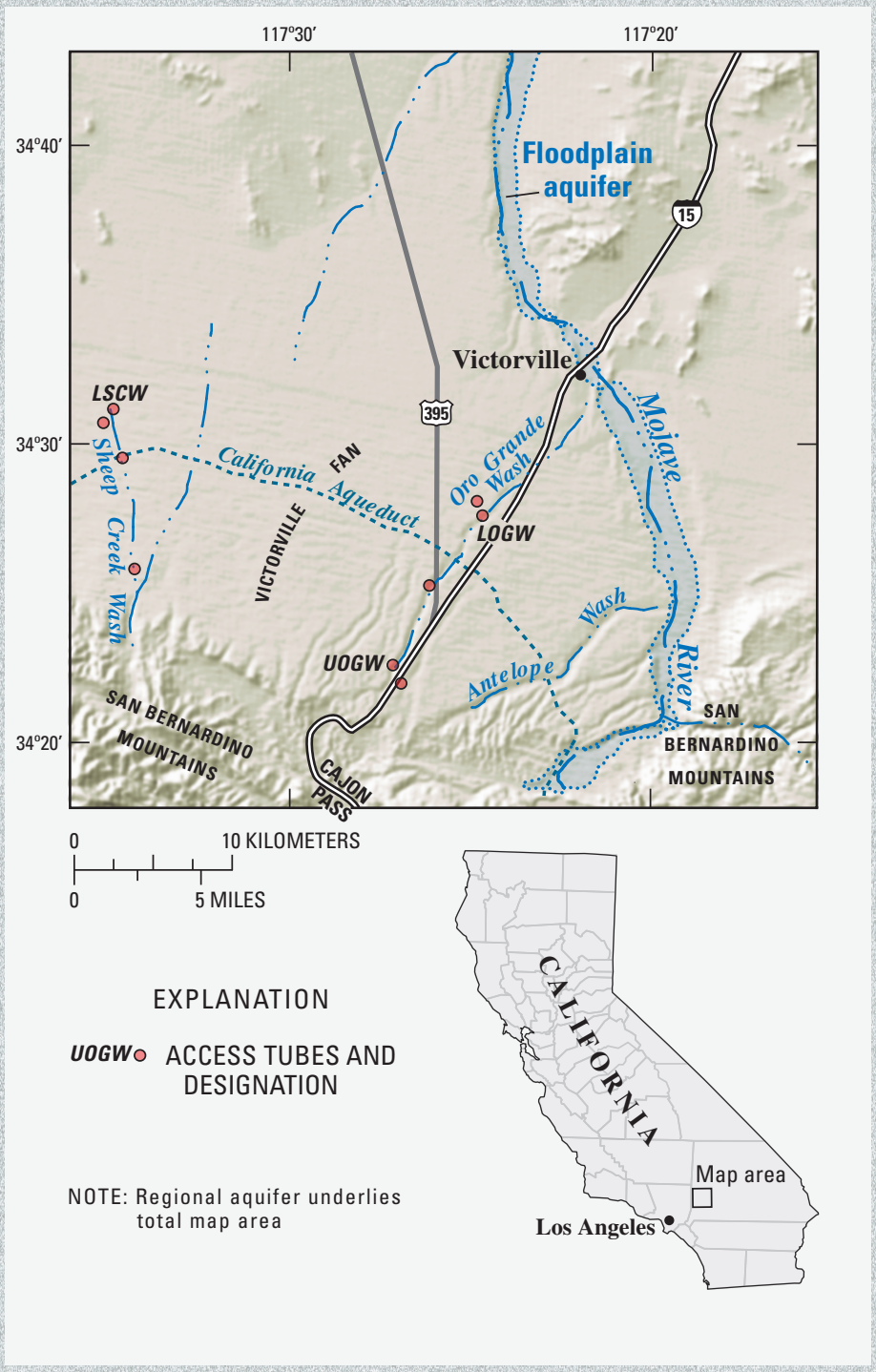

Figure 10. Location of artificial recharge pond along Oro Grande Wash, western Mojave Desert near Victorville, Calif.

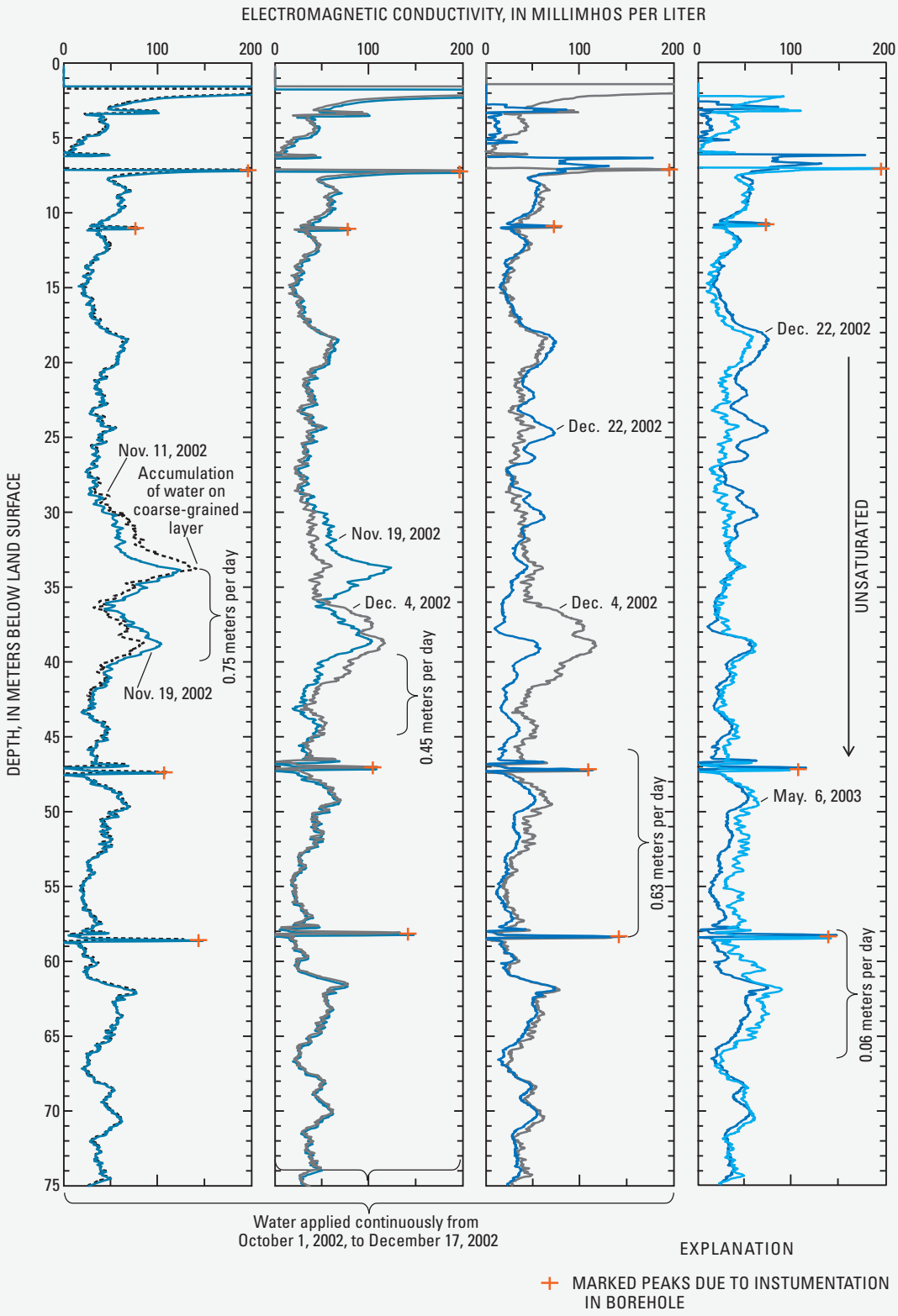

Figure 11. Selected electromagnetic logs measured from a plastic access tube emplaced within an instrumented borehole next to an artificial recharge pond near Oro Grande Wash, western Mojave Desert (near Victorville, Calif.) November 11, 2002, to May 6, 2003.

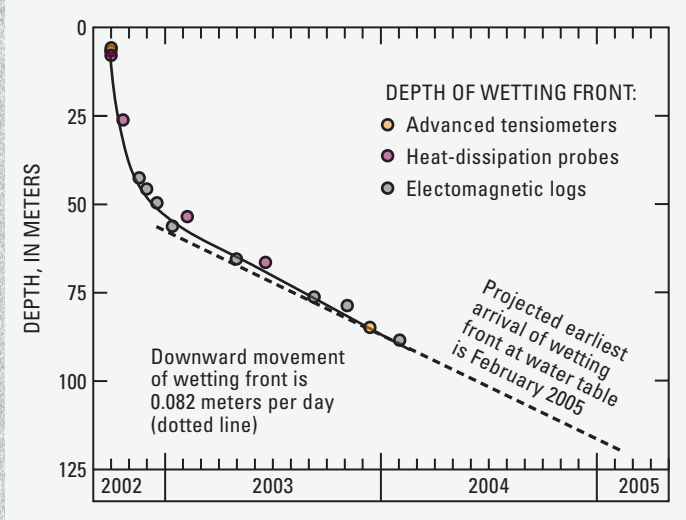

Figure 12. Downward movement of wetting front at an artificial recharge pond near Oro Grande Wash, western Mojave Desert near Victorville, Calif.

Electromagnetic Induction as a Reconnaissance Tool to Map Recharge

By Bridget R. Scanlon

This study was conducted to evaluate the potential of surface-based electromagnetic (EM) induction as a reconnaissance tool to map recharge areas at a site 120 km southeast of El Paso, Texas, in the Chihuahuan Desert (fig. 13; Scanlon and others, 1999). Because EM induction measures the apparent electrical conductivity (EC_a), which varies with clay content, water content, and salinity, it may be able to map recharge indirectly through relationships between recharge and one of these parameters. For example, Cook and Kilty (1992) showed a correlation between recharge and EC_a that was controlled by clay content. Other studies have shown a correlation between high chloride concentrations in pore water with high evaporative concentration in areas of low recharge (Scanlon, 1991; Phillips, 1994; Tyler and others, 1996). Despite the promise of EM induction methods for identifying areas of relatively high recharge, the possibility of conflicting multiple influences on the EM response must be considered for each site.

To evaluate the potential of EM induction for mapping recharge, we first need to determine what parameter exerts a controlling influence on the EM response for a given site. Then we need to assess the hydrologic significance of that parameter relative to recharge. In this study, surface-based EM transects were conducted with EM31 and EM38 meters (Geonics Inc., Mississauga, Canada) from a playa to an interplaya setting and across a fissure (fig. 13). The playa is characterized by lacustrine clay sediments whereas the adjacent interplaya is a sand-dune setting. Previous studies in the High Plains have shown that playas focus recharge (Wood and Sanford, 1995; Scanlon and Goldsmith, 1997). The fissure (640-m long) consists of an alignment of discontinuous surface collapse structures underlain by a fracture. Water ponds occasionally on this structure, possibly inducing focused recharge. In addition to the EM transects, boreholes were drilled and sampled for clay, water, and chloride contents.

The playa has higher EC_a values than the interplaya sand sheet setting due to 50 percent higher water content and 60 percent higher clay content (figs. 14 and 15A). Higher water contents in the playa sediments could reflect higher recharge through the playa or may simply be related to higher clay content within the playa. In this case, there is a high correlation coefficient (r) between the water and clay contents in samples collected in a profile adjacent to the playa (GL 4, $r^2 = 0.97$, fig. 15B). This indicates that the variability in water content can be explained entirely by variations in water storage associated with differing clay contents and is not related to recharge. Therefore, mapping EC_a with surface EM in this region would not be an effective approach to mapping recharge.

The EC_a was higher in the fissure relative to the adjacent sediments in several transects (fig. 16). The fissure sediments are characterized by lower weighted average chloride content, higher water content, and higher clay content than the adjacent sediments.

The higher water content and lower chloride content indicate the presence of focused flow beneath the fissure. The increased water content and increased clay content tend to increase EC_a, while the decreased chloride concentration tends to decrease EC_a. Increased clay contents are generally associated with lower recharge. Decreased chloride concentration suggests increased recharge. As discussed above, increased water content can indicate higher recharge or higher clay content. In this case, higher water contents in the fissure reflect higher recharge as shown by lower weighted average clay contents in profiles beneath the fissure relative to those adjacent to the fissure (Scanlon and others, 1999). In addition, considering all paired profiles (fissure versus nonfissure) with similar clay contents, there are higher water contents beneath fissures than adjacent to the fissures. Therefore, the high EC_a values in the fissure are primarily due to increased water content that reflects higher recharge in the fissure, and not simply variations in clay content. The EC_a value is not well correlated with the chloride content because water contents in areas of high chloride are too low for electrolytic conduction.

The results of this study indicate mixed utility of EM induction for mapping recharge. Areas where EC_a is controlled by clay content may be hydrologically significant if clay content controls infiltration and recharge (Cook and Kilty, 1992). However, in this study variations in clay content do not play a significant role in controlling recharge. Correlations between EC_a and water content are difficult to interpret—in many cases they simply reflect variations in clay content because clay and water contents are codependent, such as in the playa-interplaya setting. Higher water contents in the fissure were related to higher recharge. Differences in chloride content are extremely valuable in delineating water flux in unsaturated systems because chloride is readily leached in zones of high recharge and accumulates in areas of low recharge. In fact, chloride is a much more accurate indicator of high recharge than water content because of the complexities of clay-water content codependence. Unfortunately, high water flux is associated with high water content, which contributes to high EC_a, while low chloride content leads to low EC_a. Therefore, the effects of water content and chloride content counter each other, potentially limiting the effectiveness of monitoring of recharge with EM methods. As a result of the competing influences of salinity, water content, and clay content on the response EM instruments, the utility of EM methods for recharge monitoring must be assessed on a site by site basis.

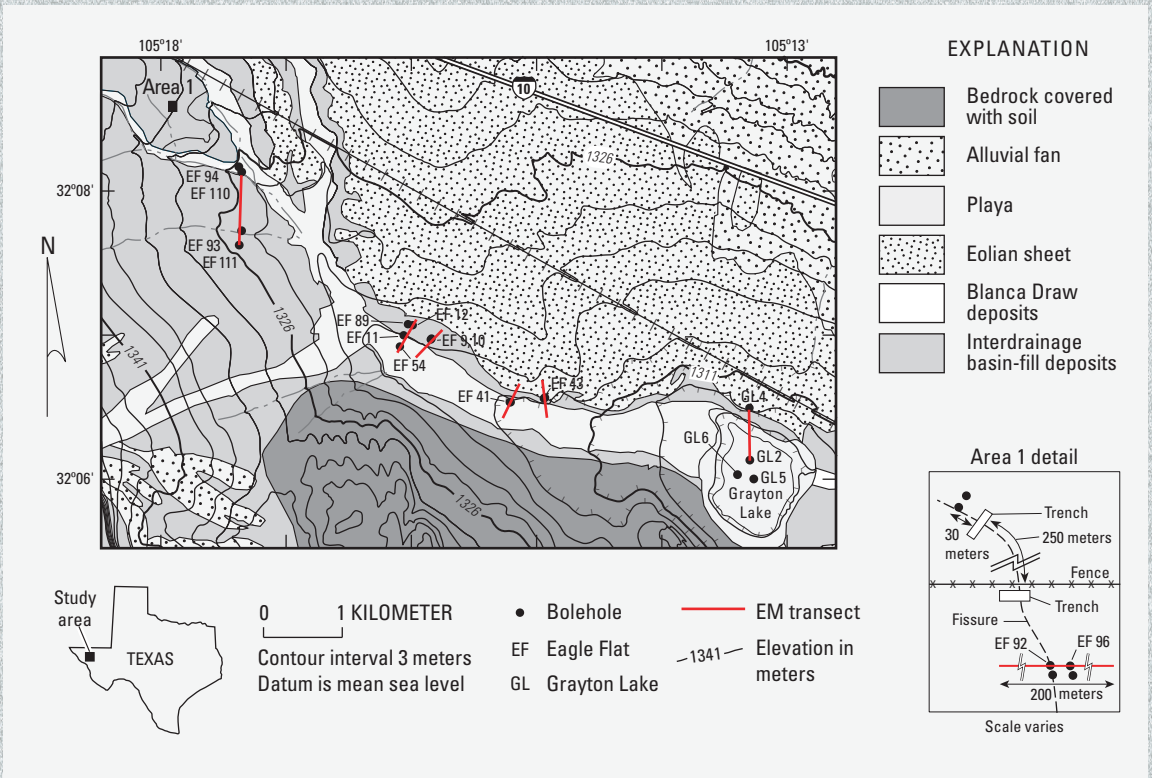

Figure 13. Location of electromagnetic (EM) induction transects and sampled boreholes relative to surface geomorphic settings in Eagle Flat Basin. Adapted from Scanlon and others (1999).

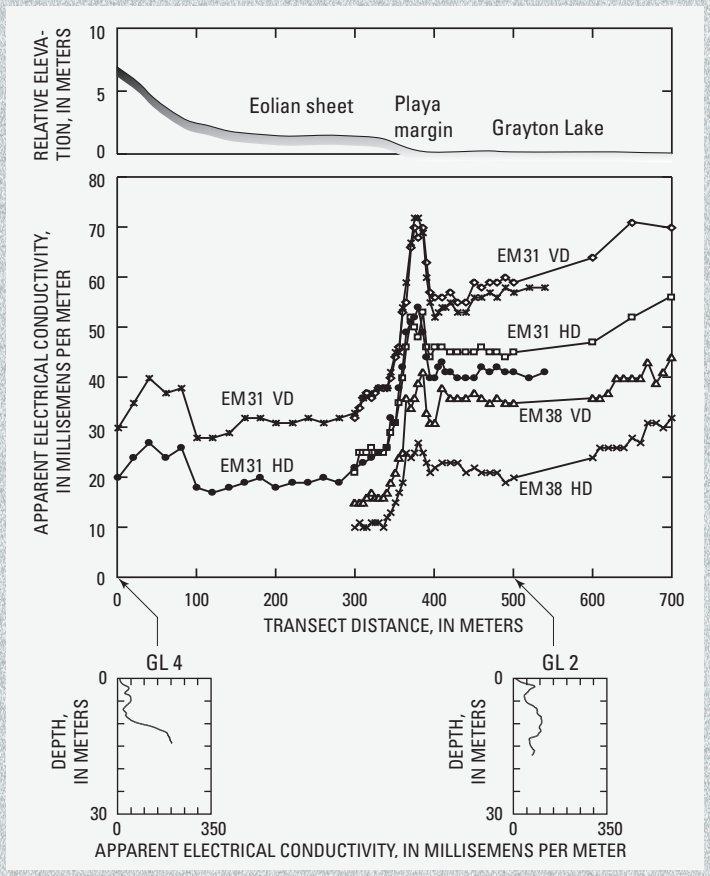

Figure 14. Variations in apparent electrical conductivity (EC_a) along a horizontal transect from the sand sheet to the playa measured with model EM31 and EM38 conductivity meters, and in a vertical profile in boreholes GL4 and GL2 measured with a model EM39 meter. Horizontal-transect EC_a was determined using vertical and horizontal dipole configurations (VD and HD). Adapted from Scanlon and others (1999). See figure 13 for locations.

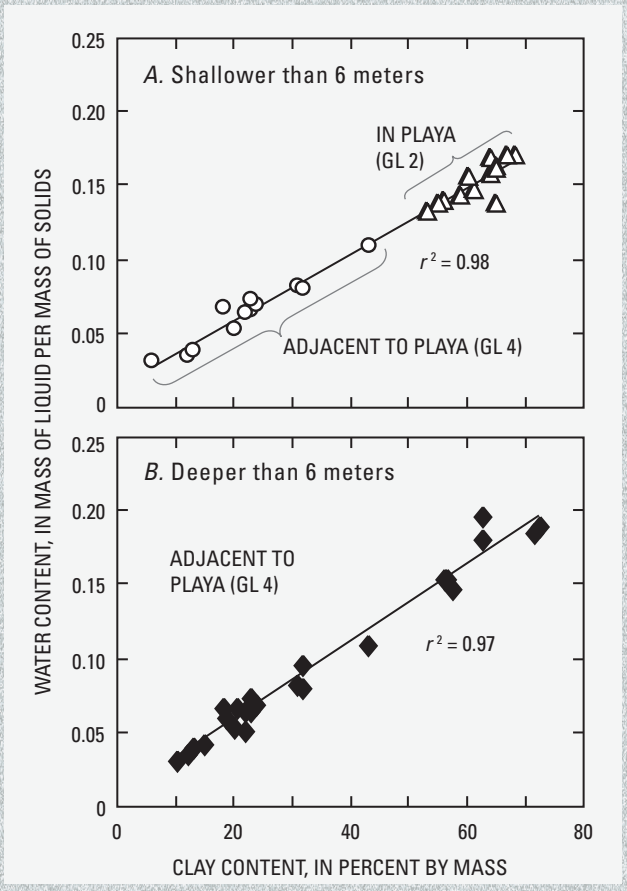

Figure 15. Relationship between water content and clay content: *A*, in the uppermost six meters (holes GL2 and GL4; *B*, deeper than six meters. The square of the correlation coefficient (r^2) indicates the fraction of variation accounted for by each line. Adapted from Scanlon and others (1999). See figure 13 for locations.

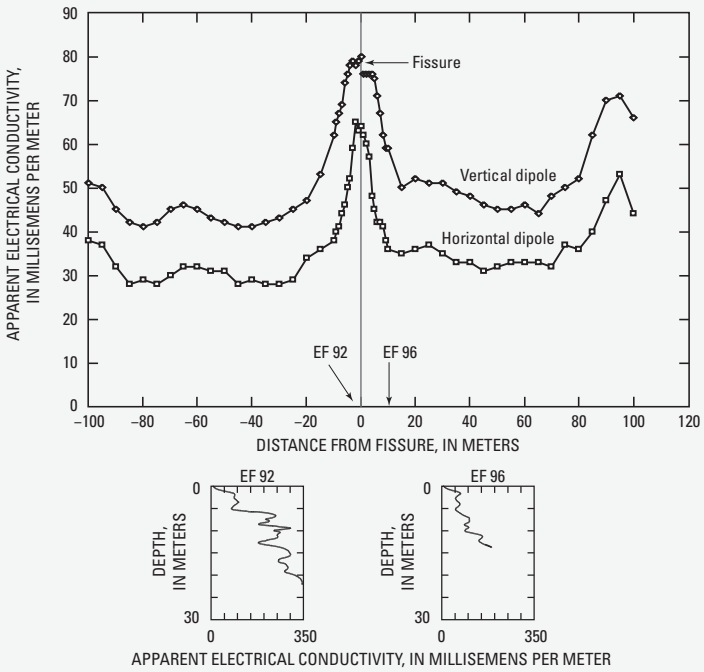

Figure 16. Variations in apparent electrical conductivity across and adjacent to a fissure, measured on land surface with a model EM31 meter in vertical- and horizontal-dipole modes, and down hole with the EM39 meter. Borehole EF92 is in the fissure; EF96 is ten meters away. Adapted from Scanlon and others (1999). See figure 13 for locations.

controlled by geology) gravity monitoring has limited use for subsurface water content mapping.

Recently, however, the value of time-lapse gravity surveys has been recognized for inferring changes in subsurface water content distributions. This use of gravity methods relies on the fact that, in most environments, changes in subsurface mass through time are dominated by changes in water storage. Therefore, after standard corrections are applied for tidal and instrument effects, the change in gravitational attraction at the ground surface can be related to the cumulative change in the water stored in the subsurface. Gravity-based water storage change monitoring has great promise for water balance applications because the method is portable, rapid, and requires far less infrastructure than monitoring wells. However, the method does not provide measurements of the subsurface water distribution. In fact, the method may be susceptible to errors if water accumulates at shallow depths above the water table, due to the inverse dependence of gravitational attraction on the distance to a body. Despite this potential error, gravity-based methods are uniquely capable of providing spatial estimates of water storage change over large areas. As a result, they will likely see expanded use both for direct estimation of water storage change and for calibration of saturated flow models. An example of the direct use of time-lapse gravity for monitoring changes in water storage throughout a basin is provided in "Monitoring temporal changes in water storage with gravity."

Hydrogen Density

One borehole logging technique has shown particular promise for recharge monitoring—neutron logging. Neutron probes emit epithermal neutrons produced from a radioactive source. These neutrons enter the medium surrounding the borehole, where they collide with the constituents of the medium. Because neutrons and hydrogen atoms have similar masses, collisions of epithermal neutrons with hydrogen atoms cause a relatively large loss of energy. Many such collisions "thermalize" (slow) the emitted neutrons. By counting the rate of thermalization of the emitted neutrons, the hydrogen density of the medium can be inferred. In the absence of neutron capturing elements, neutron counts are well correlated with the volumetric water content of the medium in close proximity to the borehole. Neutron probes are unique among water content profiling methods in their ability to measure to great depths. This ability is due to the location of both the neutron source and the detector in the probe body, requiring only a one-way information link with the surface. However, the placement of the radioactive source in the borehole is also a primary limit on the widespread, continuing use of neutron methods due to regulatory and liability considerations. In addition, because neutron methods use a radioactive source, measurements must be made over relatively long times (0.5 – 1 minute per measurement point). This measurement time is fast enough to track slow recharge, but may not be sufficiently rapid to characterize rapid processes near the ground surface. Furthermore, due to neutron loss across the ground surface and to safety

considerations, neutron methods are not typically used at or near the ground surface. Due to their unrivaled ability to profile the water content to great depths in a single borehole, it is likely that neutron probes will remain a standard method for measuring water content profiles to calibrate unsaturated flow models. The case study "Estimating recharge using time-lapse neutron moisture logging" is provided as an example of the unique abilities of neutron probes for episodic recharge monitoring.

Well Logging

Many borehole-logging techniques have been developed for oil and mineral exploration (Labo and Mentemeier, 1987; Kearey and others, 2002). Most of these methods are aimed at defining either geologic structure or fluid distributions, both of which may be adopted for similar uses for recharge monitoring. Borehole logging techniques typically give high-resolution depth-continuous measurements at a limited number of locations. The utility of borehole geophysical methods is commonly increased through simultaneous interpretation of multiple methods. Similarly, borehole methods are useful for constraining the interpretation of surface-based geophysical methods. Borehole geophysical measurements are often conducted in boreholes upon completion. It is likely that this information could be used more routinely and more completely to characterize the spatial structure of the chemical, physical, and hydraulic properties within the unsaturated zone. At a minimum, these data should be used to identify those areas that may impact water flow and solute transport to ensure that more-detailed measurements are made in critical zones. This would represent a first step toward the use of geophysical methods to optimize the design of monitoring networks for recharge monitoring.

Standard texts provide descriptions of the full range of well logging methods (for example, Desbrandes and Brace, 1986; Keys, 1990; Telford and others, 1990). Neutron logging and electromagnetic-induction logging were already discussed in connection with the mapping of fluid distributions. An illustration of the combined use of neutron and electromagnetic-induction logging to define geologic structure appears in the case study "Geophysical well-logging to estimate subsurface physical and hydraulic properties."

Closing Remarks—A Conceptual Framework for Applying Geophysics to Recharge Monitoring

Geophysics has much to offer to the characterization of the rates, timing, and patterns of recharge. Gravity could be used directly by water resource planners to monitor water storage changes in time. Temperature monitoring and self potential methods may allow for direct measurement of water fluxes in the subsurface, offering the possibility to quantify recharge locally. Seismic and well-logging methods can be used to build more accurate representations of subsurface hydrogeologic structure. Borehole ground penetrating radar, neutron probes, and borehole electromagnetic induction, and point methods like TDR and capacitance probes allow for detailed monitoring throughout the unsaturated zone, improving the calibration of unsaturated flow models and thereby advancing our understanding of the linkages between unsaturated zone processes and recharge. Finally, a suite of electromagnetic methods allow for coarse-scale monitoring of unsaturated zone processes throughout a basin, allowing for better identification of critical areas within a basin that require more intensive characterization.

The key to the successful use of geophysics in recharge investigations is the identification of the appropriate geophysical method or methods for specific hydrologic monitoring needs. The choice of monitoring method must begin with the eventual application in mind. That is, what will be the primary use of the geophysical data? Possible uses include definition of the hydrogeologic structure of the subsurface for basin scale saturated flow models or for more localized unsaturated flow models, estimation of recharge for use in saturated flow models, testing of conceptual models of unsaturated flow, and identifying critical areas for traditional hydrologic monitoring efforts. It is critical that hydrologic insight be used to identify these key processes for a particular investigation. Once the eventual uses of the geophysical data are identified, available geophysical methods should be analyzed quantitatively to address two questions. First, is the method likely to have sufficient sensitivity to the key hydrologic parameters of interest to help resolve the hydrologic question? Second, is the method likely to produce data with sufficient spatial and temporal resolution for accurate hydrologic analysis? These questions can only be addressed confidently through the application of geophysical insight, through the direct participation of someone who is familiar with the application of geophysics to hydrologic problems. The optimal use of geophysics in hydrologic studies will likely require the increased use of geophysical forward models to predict instrument response for expected hydrologic conditions. Ideally, these models should be integrated with standard numerical flow models to encourage the routine use of geophysical tools in hydrologic investigations. The case studies presented here have shown just a few examples of the promises and pitfalls of geophysical methods for recharge monitoring. The common lesson is that measurement methods can only be successful if they are applied to appropriate problems. Eventually, all monitoring methods (traditional hydrologic methods, geochemical methods, and geophysical methods) should be considered in a common cost-benefit framework, balancing the capital and labor costs of measurement methods with their likely benefits in terms of reduced uncertainties in hydrologic analyses. This will allow for the design of an optimal mixture of methods to address a given problem within an available budget. This holistic, integrated view of the role of measurement in hydrology provides an effective conceptual framework for applying geophysics to recharge monitoring.

Monitoring Temporal Changes in Water Storage with Gravity

By Donald R. Pool

Gravity methods were used to monitor ground-water storage and estimate magnitudes and distributions of recharge in a 141 km^2 region in the foothills of the Santa Catalina Mountains, Tucson, Ariz., from summer 1999 through winter 2002. Several ephemeral streams discharge from the crystalline rocks, cross the area in incised channels, and discharge to Rillito Creek and other tributary channels (fig. 17). Tertiary sediments of low to moderate permeability have been exposed by incision of the current drainage system. However, narrow stringers of highly

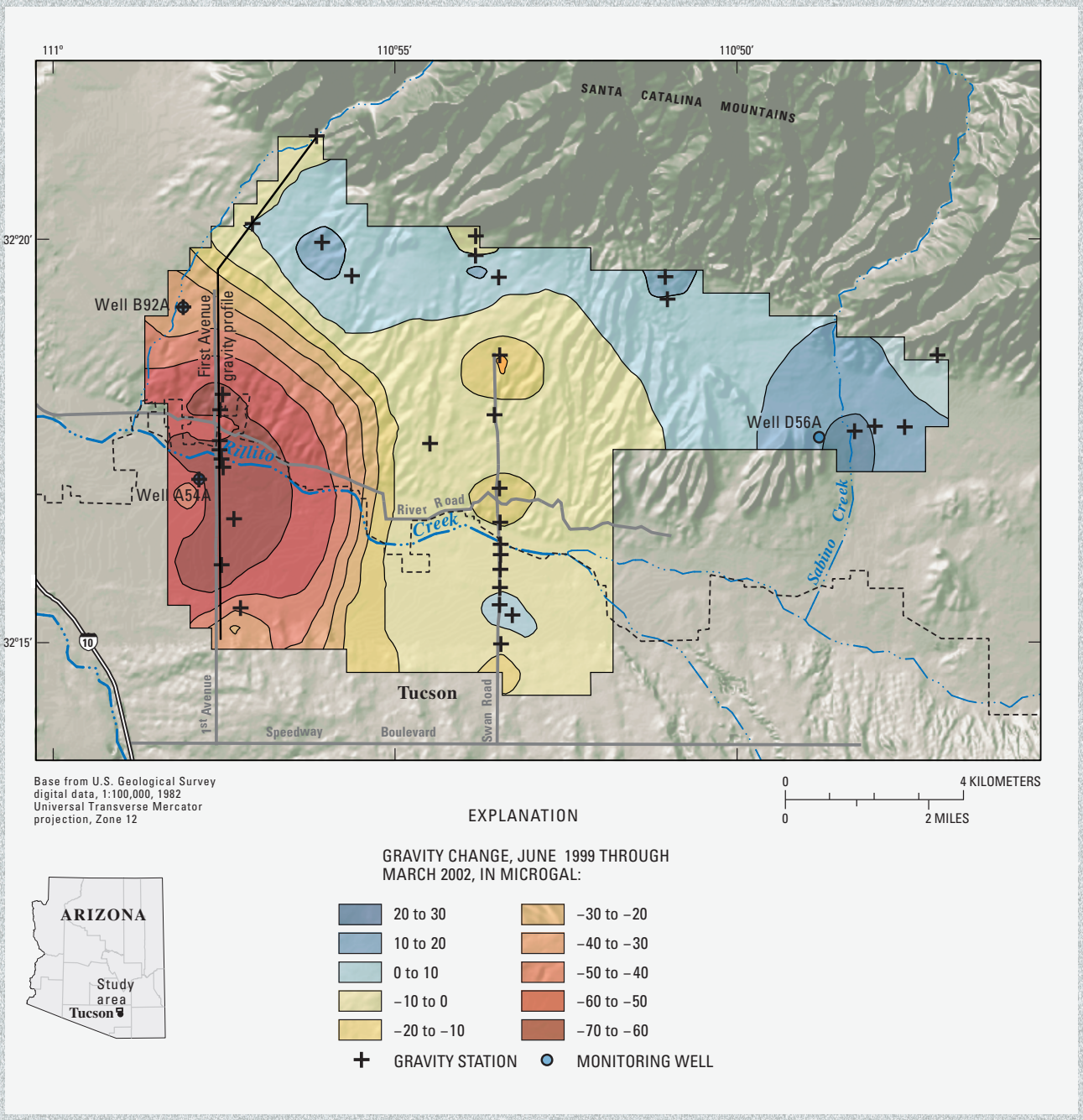

Figure 17. Location of gravity-network stations and changes in gravity, June 1999 through March 2002, near the foothills of the Santa Catalina Mountains, Tucson, Ariz.

permeable alluvium occur along the stream channels and may accept and store significant amounts of streambed infiltration. Ground water is removed from the aquifer through ground-water withdrawals, evapotranspiration, and ground-water flow out of the study area. Ground-water withdrawals and evapotranspiration within the study area are small, however, in comparison to ground-water flow across the area boundary. Ground-water primarily flows toward a major area of ground-water withdrawal south of Rillito Creek and outside of the study area.

The foothills gravity-station network included 23 stations. Two stations were on crystalline rock at the base of the mountains where ground-water storage and gravity change should be minimal. One of the stations on crystalline rocks was also a gravity reference station where the absolute acceleration of gravity was measured six times during the study by the National Geodetic Survey. Gravity at each station was measured relative to the reference station nine times between June 1999 and March 2002. Few wells are available for water level monitoring in the area because few water supply wells have been drilled in the relatively low-permeability saturated-zone materials. Water levels were measured at monitoring wells shown on figure 17.

The general distribution of gravity changes during the study period included an area of decline of up to 60–70 microgal along the lower reaches of Rillito Creek and a swath of increased gravity (up to 10–20 microgal) along the base of the Santa Catalina Mountains (fig. 17). The largest increase in gravity was measured near Sabino Creek, the largest drainage from the mountains. The distribution of gravity change was dominated by declines due to ground-water flow out of the study area and increases due to periodic streamflow infiltration along the major ephemeral channels. Increased storage resulted from precipitation and streamflow infiltration that primarily occurred during two periods, summer of 1999 and July through October of 2000 (fig. 18). Three water-level hydrographs display representative variations in water-level response to infiltration and recharge (fig. 18). Two of the wells, B-92A and A-54A, display water-level declines of 1 to 3.5 m resulting from ground-water withdrawals outside of the study area. High rates of water-level decline along Rillito Creek also resulted from redistribution of recharge that occurred during the winter of 1998. Well D-56A is far from major areas of ground-water withdrawal and displayed slight water-level increases during the period. Gravity change during the period displays a pattern similar to the water levels. Major periods of infiltration and recharge were followed by water-level recovery or significantly reduced rates of water-level decline near major ephemeral streams (wells D-56A and A-54A). Gravity increases also occurred at most stations following major periods of infiltration and recharge.

The distribution of gravity change was monitored in detail along two profiles across Rillito Creek (fig. 17) to assess the redistribution of infiltrated water following major streamflow. Distributions of subsurface storage change in the unsaturated and saturated zones across a profile along First Avenue were simulated with a 2-dimensional gravity model that applies the algorithm of Talwani and others (1959; fig. 19). Constraints on the interval of saturated storage change were available from water levels at several wells. Changes in gravity were defined by surveys on June 25 and August 18, 1999, which included a period of high precipitation and streamflow. Changes along the profile indicate that increases in gravity of 30 to 70 microgal near the stream channel were superimposed on a regional trend of declining gravity (fig. 19). Increases occurred near Rillito Creek and near the mountains. A portion of the gravity change near the stream was attributable to a rise in the water table of a few meters at well North First. The remaining gravity increase was caused by increased storage in the unsaturated zone. The lateral extent of the unsaturated zone storage increase is well constrained by the distribution of gravity stations. The model assumes saturated zone storage change near the Santa Catalina Mountains; however, the vertical distribution of storage change within the saturated and unsaturated zones in the area cannot be separated because no water-level data are available. Gravity decline of less than 10 microgal at most wells distant from the stream channel were simulated adequately by using the measured water-level decline and assuming a specific yield of 0.27. Gravity decline of 10 to 30 microgal at wells A-54A and B-92A, however, were larger than could be explained by the observed water-level change. Significant storage change in the unsaturated zone was therefore required at these wells to simulate the observed gravity change.

The volume of ground-water storage change for the monitored period within the study area was estimated by integration of the linearly interpolated gravity changes across the study area and applying the excess-mass equation (Telford, 1990). Storage change since June 1999 was calculated for gravity surveys done in August 1999, January 2000, June 2000, November 2000, March 2001, and March 2002 (fig. 20). Total ground-water storage for the study area increased more than 25 million cubic meters (Mm^3) following July 1999 and generally decreased thereafter to a total loss of more than 40 Mm^3. Storage changes in the Rillito Creek and foothills subareas displayed somewhat different trends. The foothills subarea comprised most of the increase following July 1999, 20 Mm^3, and displayed continuous declines thereafter. The Rillito Creek subarea displayed a smaller increase following July 1999 and slight increases in storage following October 2000 with declines through the rest of the monitoring period.

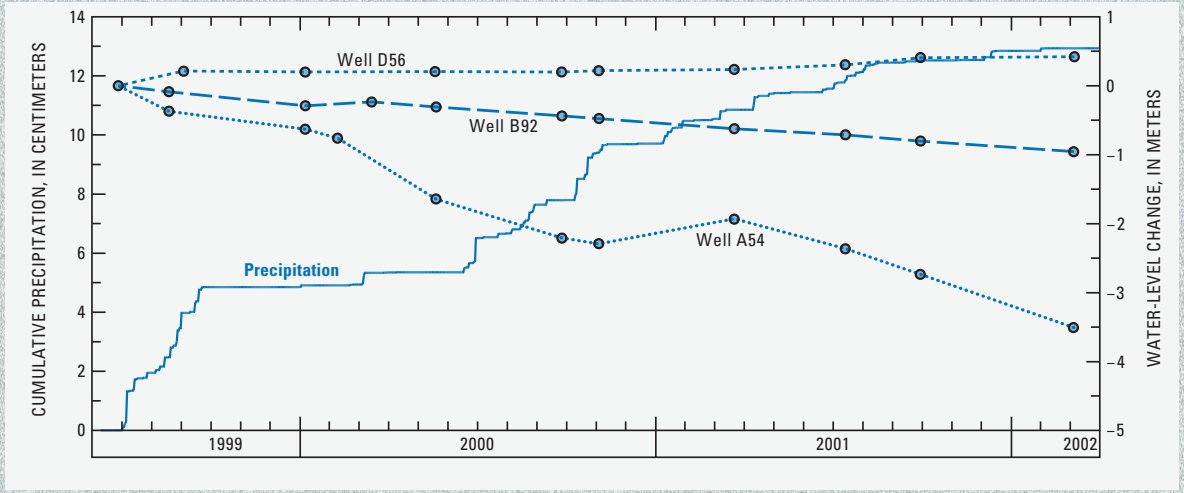

Figure 18. Cumulative precipitation and water levels in selected wells, June 1999 through March 2002, near the foothills of the Santa Catalina Mountains, Tucson, Ariz.

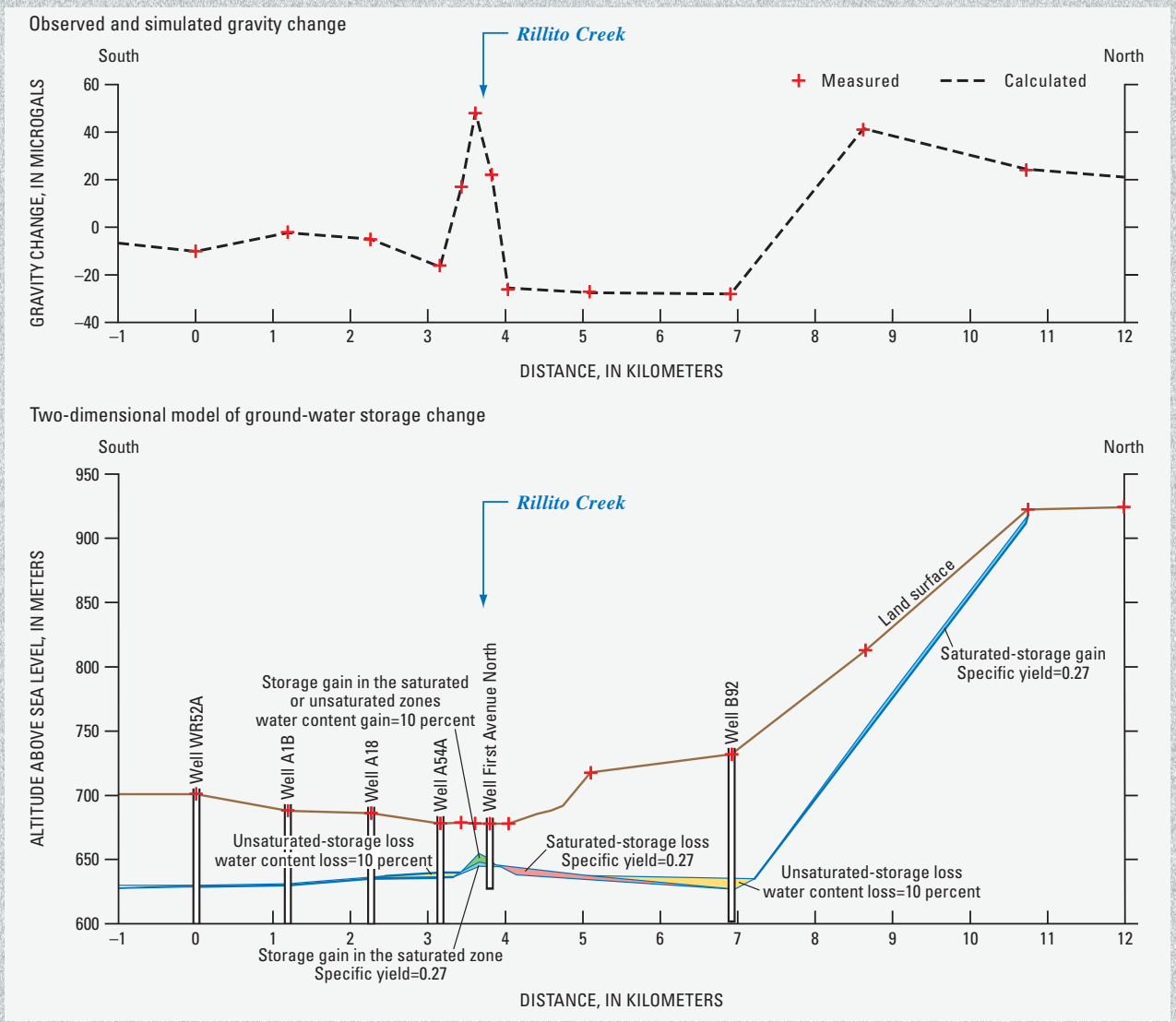

Figure 19. Two-dimensional simulation of ground-water storage change along First Avenue, June 24 to August 17, 1999, near the foothills of the Santa Catalina Mountains, Tucson, Ariz.

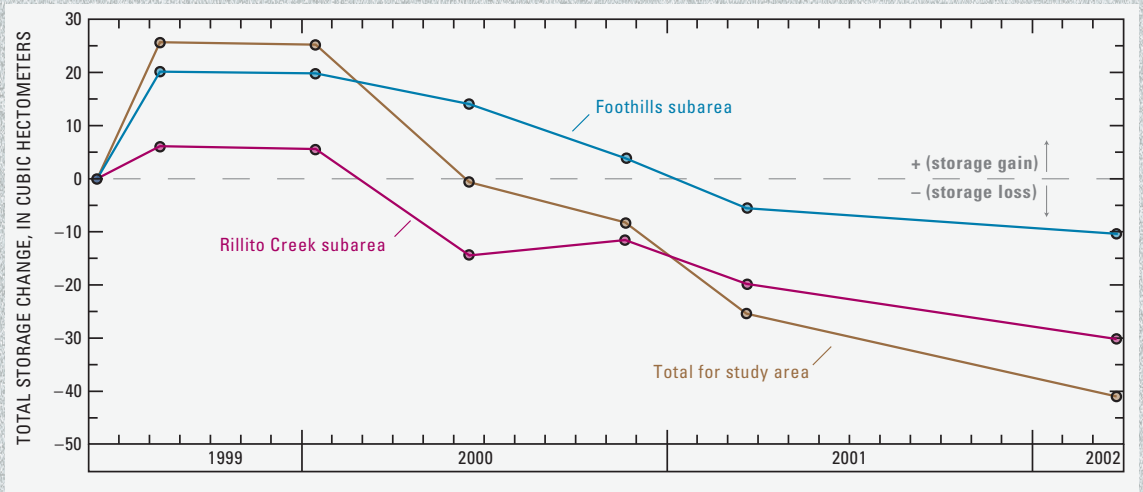

Figure 20. Total storage change in the foothills of the Santa Catalina Mountains, June 1999 through March 2002, Tucson, Ariz. Total for study area is the sum of Rillito Creek and foothills subareas.

Estimating Recharge using Time-Lapse Neutron Moisture Logging

By Alan L. Flint and Lorraine E. Flint

Spatially distributed recharge from natural precipitation was estimated by measuring soil-water-content profiles at Yucca Mountain, southern Basin and Range, Nevada. Soil-water contents were determined with moisture meters containing an americium-beryllium neutron source (model CPN-503, Campbell Pacific Nuclear, Martinez, Calif.; Flint and others, 2001). Profiles were measured in 100 boreholes for up to ten years by using field- and laboratory-calibrated neutron-moisture meters. The boreholes ranged in depth from approximately 10 meters to 84 meters. Water-content profiles were measured regularly—on a monthly basis and more frequently after major rainfall events (Flint and Flint, 1995). These measurements were used to help develop conceptual models of the mechanisms of recharge in various topographic settings.

One method of interpretation of the water content profiles was to identify the depth of the wetting front as a function of time following a precipitation event. The wetting front depth can be determined by statistical analysis of a time series of water content profiles. Due to the random radioactive decay from the neutron source, the smallest resolvable variation in water content is about 0.01 m^3/m^3 (Hignett and Evett, 2002). The depth below which the measured water content changes with time are less than this threshold can be associated with the depth to which water has infiltrated. Data collected during a ten-year period show that, on the basis of this criterion, infiltration never reached depths greater than five meters in the thick alluvium at the location shown in figure 21.

Examination of a time series of water content profiles provides additional insight into the infiltration, redistribution, and recharge processes. A ten-year series of water content profiles was collected in a site located in a wash with 8 m of alluvium overlying a nonwelded volcanic tuff (fig. 22). The borehole was installed in 1984, several weeks after a major runoff event. Water drained from the alluvium and the underlying tuff during the next several years. Several minor runoff events occurred in the mid 1980s, followed by dry conditions persisting throughout the drought of 1989 and 1990, followed by El Niño period runoff events in 1991 and 1992. Even these large events do not show measurable increases in water content below three meters, indicating that evapotranspiration could easily remove the infiltrated water before it became recharge. In contrast, the 1995 El Niño runoff event caused significant infiltration below the zone of evapotranspiration, eventually resulting in recharge.

The previous analyses use relative measures of water content change to identify the maximum depths of infiltration. These can be achieved without the need for soil-specific calibrations. More-quantitative assessments of infiltration flux require calibration to determine the volumetric water content from neutron counts. As an example, neutron counts, measured in a 79-m borehole drilled through alluvium and several different types of tuffaceous rock, are compared with laboratory-measured water contents from rock cores (fig. 23*A*). A linear correlation between counts and volumetric water content has a square correlation coefficient (r^2) of 0.88, a root-mean-square error of 0.036, and a measurement repeatability of 0.01. The laboratory- and field-measured water content profiles compare well except at the surface (fig. 23*B*). This discrepancy is likely due to the effects of large changes in

water content with depth in this region and uncertainty regarding the averaging of water contents within the vertical sampling interval (approximately 0.5 m; Klenke and Flint, 1991).

The ability to measure changes in volumetric water content with time to great depths allows for the calculation of transient infiltration fluxes directly through measurements of changes in water storage. Based on the time series of water content profiles shown in figure 22, it can be argued that recharge will occur only if infiltration extends below a depth where evapotranspiration can remove all infiltrated water. Flint and Flint (2000) used measured increases and decreases in water content below the zone of evapotranspiration to determine recharge rates in a variety of topographic positions. Specifically, increased water contents below the depth of evapotranspiration were taken to represent potential recharge. Borehole UZ N-15, located in a small channel in a large flat mesa, was drilled in 1992 and flowed once during 1993 and twice during the 1995 El Niño periods (fig. 24*A*). The soil is 0.7 m thick and overlies fractured, welded tuff grading downward to a moderately welded tuff with depth. The soil-tuff interface became saturated allowing water to enter the fractured rock. The water content initially increased following each runoff event, and then drained throughout the profile. Specifically, water moved through fractures in the top 2 m of welded tuff with little imbibition into the matrix. Below 3 m, water was imbibed by the more permeable moderately welded tuff. The average water content between 2 m depth and the soil/bedrock contact increased after each event (fig. 23B). There were increases ranging from 150 to more than 300 mm of water in storage from the four infiltration events. Drainage, calculated as the slope of the line between the last El Niño event in 1993 and the first El Nino event in 1995, declined at an average rate of approximately 20 mm/yr (fig. 24*B*).

Under steady-state conditions, infiltration occurs without changes in water storage with time. Assuming a unit gradient condition, the measured water content can be used together with an independent measure of the unsaturated conductivity function (Flint and others, 1999) to calculate the steady-state flux with the Buckingham–Darcy flux law (Jury and others, 1991). This method was employed to develop the first spatially distributed map of net infiltration for Yucca Mountain, NV (Flint and Flint, 1994). More advanced analysis of water content profiles makes use of inverse hydrologic modeling to calibrate infiltration models, which in turn can be used to calculate recharge. Hevesi and others (1994) and Hudson and others (1994) used this approach to calibrate 1-dimensional models at Yucca Mountain. Eventually a series of 1-dimensional models were combined to develop a large-scale rainfall/runoff model by using runoff data and the estimated fluxes in the neutron holes (Flint and others, 1996). The calibrated model results were used to provide the upper boundary conditions for a three-dimensional site scale model of the Yucca Mountain region (Flint and others, 2001; 2002).

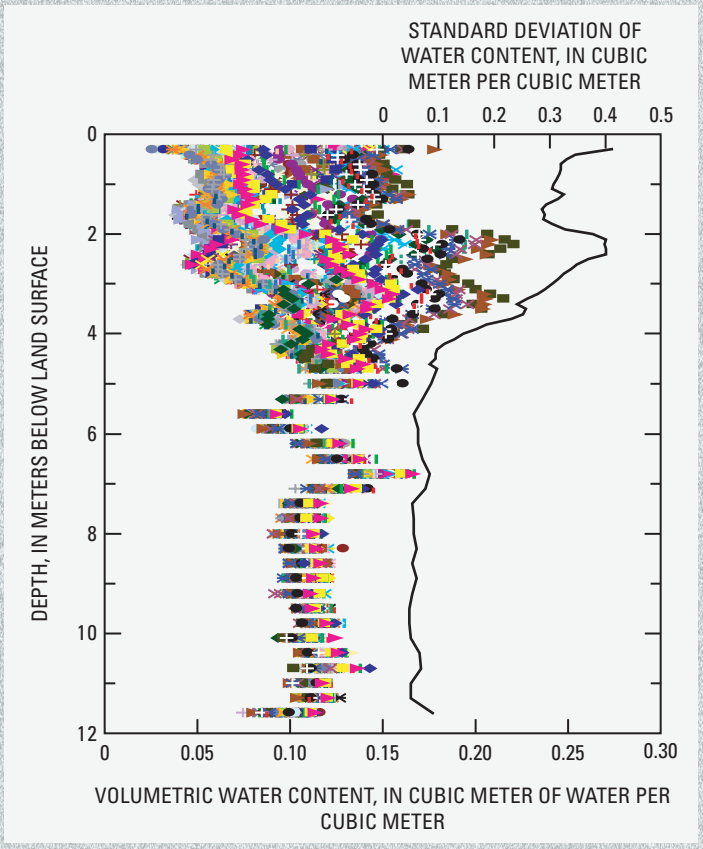

Figure 21. Volumetric water content (points) and standard deviation (curve) with depth at borehole UZN #19 for ten years of sampling during 1984–1995. Each symbol type denotes measurements from a different day.

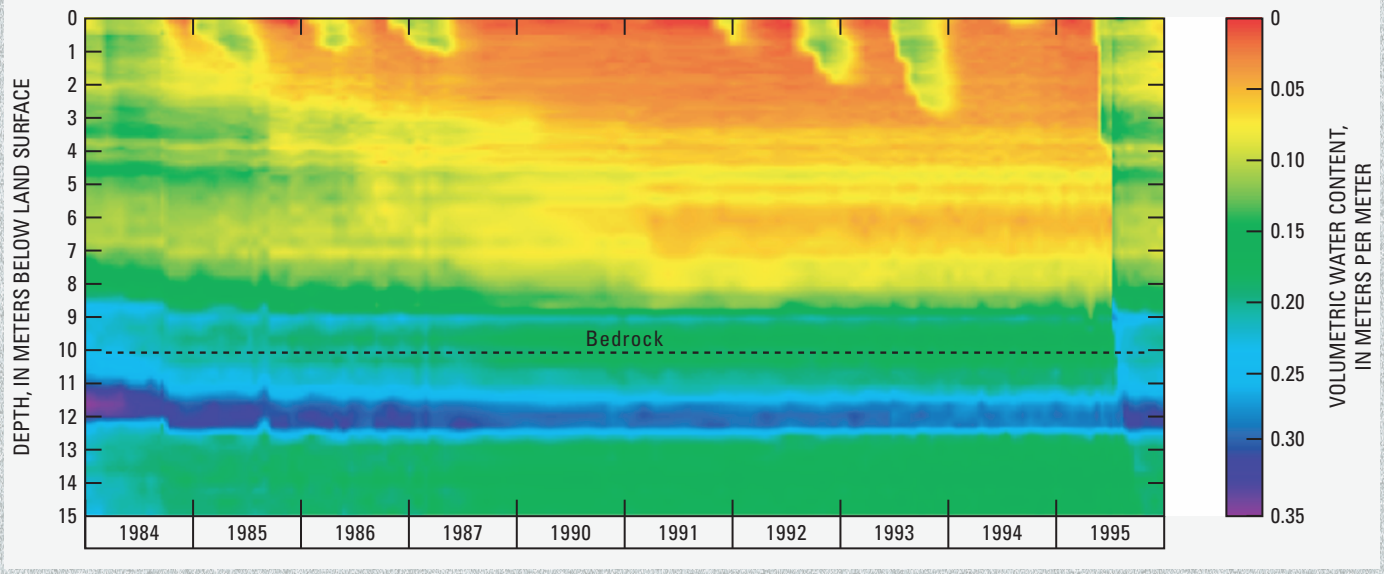

Figure 22. Volumetric water content with depth for ten years at borehole UZN #1.

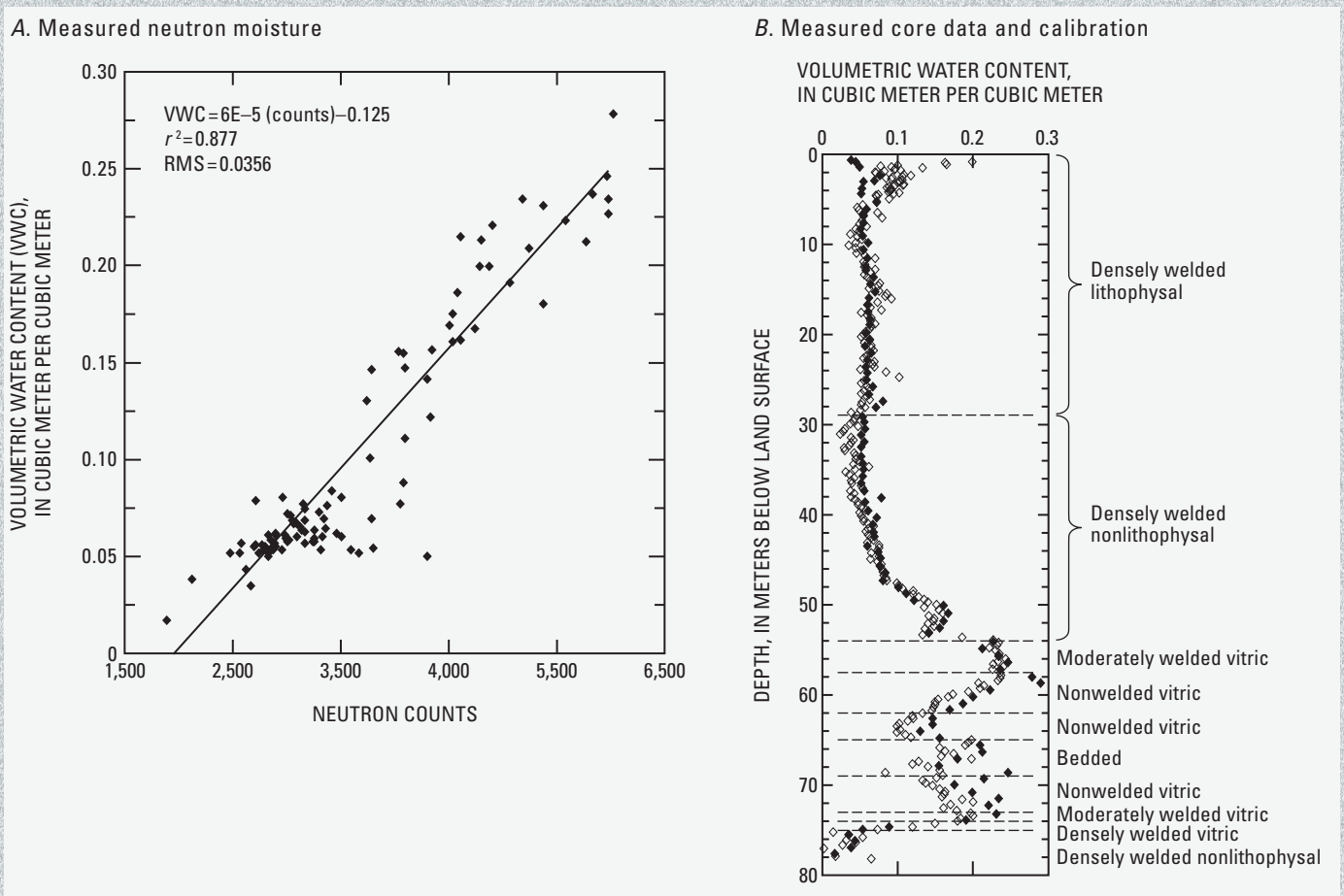

Figure 23. Neutron moisture meter calibration data included: *A,* Measured neutron moisture meter counts versus measured core data, and; *B,* Measured core data for borehole UZ N-55 (solid diamonds) and calibration equation applied to moisture meter logs (open diamonds).

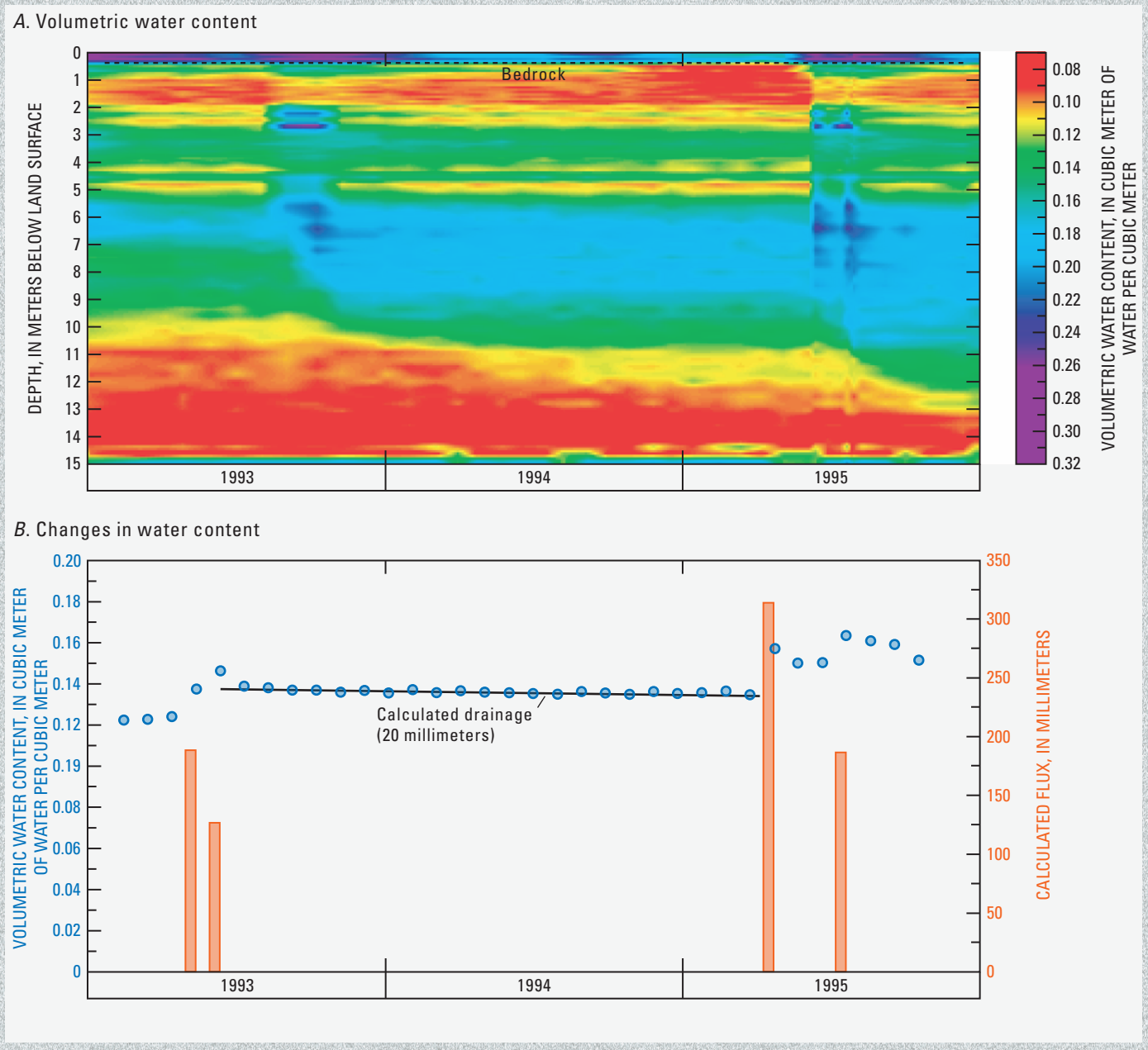

Figure 24. Application of neutron-based water-content measurements to calculate flux at borehole UZ-N15, where 0.8 meters of alluvium overlies fractured bedrock: *A,* Volumetric water content with a depth for three years, and; *B,* Changes in water content below two meters in bedrock, flux calculated from those measurements, and the drainage between rainfall events (calculated from the slope of the line).

Geophysical Well-Logging to Estimate Subsurface Physical and Hydraulic Properties

By James B. Callegary

Geophysical well-log data were collected to identify areas of active recharge and to help quantify recharge in ephemeral channels of the Sierra Vista subwatershed of the Upper San Pedro River Basin, Ariz. (fig. 25). Sixteen boreholes were drilled at 15 sites, twelve in the active portions of ephemeral stream channels and four in inter-basin sites. The boreholes in active channels were distributed among five ephemeral channels, representing the variation of tributary types found in the Sierra Vista subwatershed. All boreholes were lined with unscreened polyvinyl chloride (PVC) casing with a diameter of 0.05 meters. Most of the boreholes were completed above the regional water table. Manual estimation of the grain size distribution of cuttings was conducted in the field for each 0.3-meter depth interval. Gaps in the grain size distribution logs occur where cuttings were not retrieved or were lost. Laboratory estimates of grain size distribution were conducted on cuttings and a subset of retrieved cores in three boreholes.

Electromagnetic induction logging (EMI) was used to distinguish between clay layers and sand/gravel layers. Analyses of drill cuttings showed uniformly low chloride concentrations. Therefore, zones of increased electrical conductivity (EC) can be associated with high volumetric water content or high clay content. High neutron counts are associated with zones of high volumetric water content. As a result, the EMI and neutron results can be used together to distinguish zones of increased water content or clay-rich regions. This can be especially useful for distinguishing between zones with high water content due to high water retention associated with high clay content, and zones with high water content due to subsurface structure, such as capillary barriers.

EMI measurements were collected in all boreholes at a logging rate of 3 meters per minute. Measurements were recorded at 0.01–0.02-m intervals. Neutron soil moisture counts were measured in six boreholes. Counts were measured over a 32-second period at each depth with a 0.25-m measurement interval. Quantitative analysis of volumetric water content requires soil-specific calibration (Hignett and Evett, 2002). No calibration was performed in this investigation. Rather, the neutron responses were used as qualitative indicators of variations in water content with depth.

Data collected at Banning Creek represent the subsurface conditions of an incised, ephemeral stream channel (fig. 26). Incision of the channel near the borehole ranges from 2 to 5 meters. The channel surface is cobbly to sandy. Flows occur only after summer convective or winter synoptic scale storms. The laboratory and field grain size distributions are similar. Both grain size distribution logs show shallow and deep regions with relatively low clay fractions bounding a middle depth interval (7–17 m) that is more clay rich. Both logs also show isolated, thin

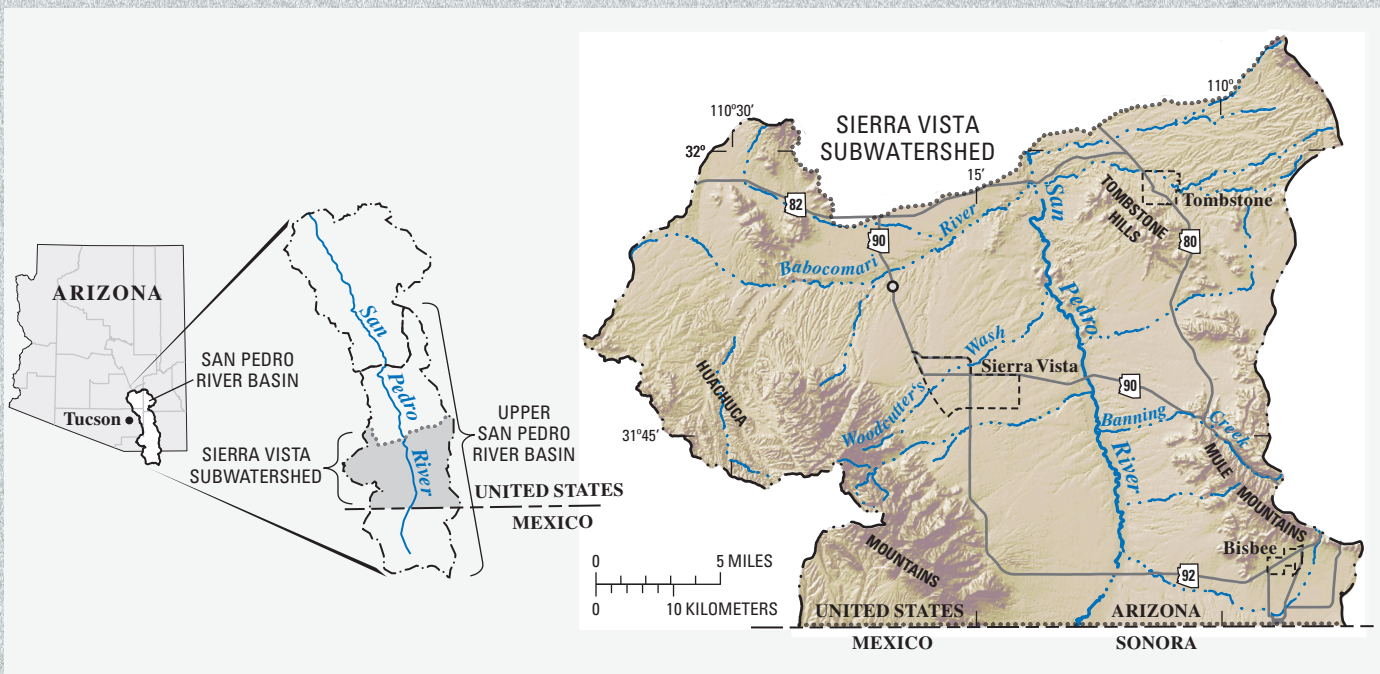

Figure 25. Location of Sierra Vista subwatershed of the Upper San Pedro River Basin, southeastern Ariz.

clay-rich zones in the shallow and deep regions. Laboratory-determined clay content tended to be lower than field estimates for depths greater than seven meters. This situation was reversed for shallower depths, where a different analyst performed the laboratory determinations. The difference may therefore reflect operator bias.

There is also general agreement between the grain size distribution logs and the EMI results. The EC is relatively high in the middle depth region compared with the shallow and deep zones. In addition, clay-rich zones at 3, 19–21, and 25 meters depth are identified. Finally, the EMI results agree with the laboratory results in identify-

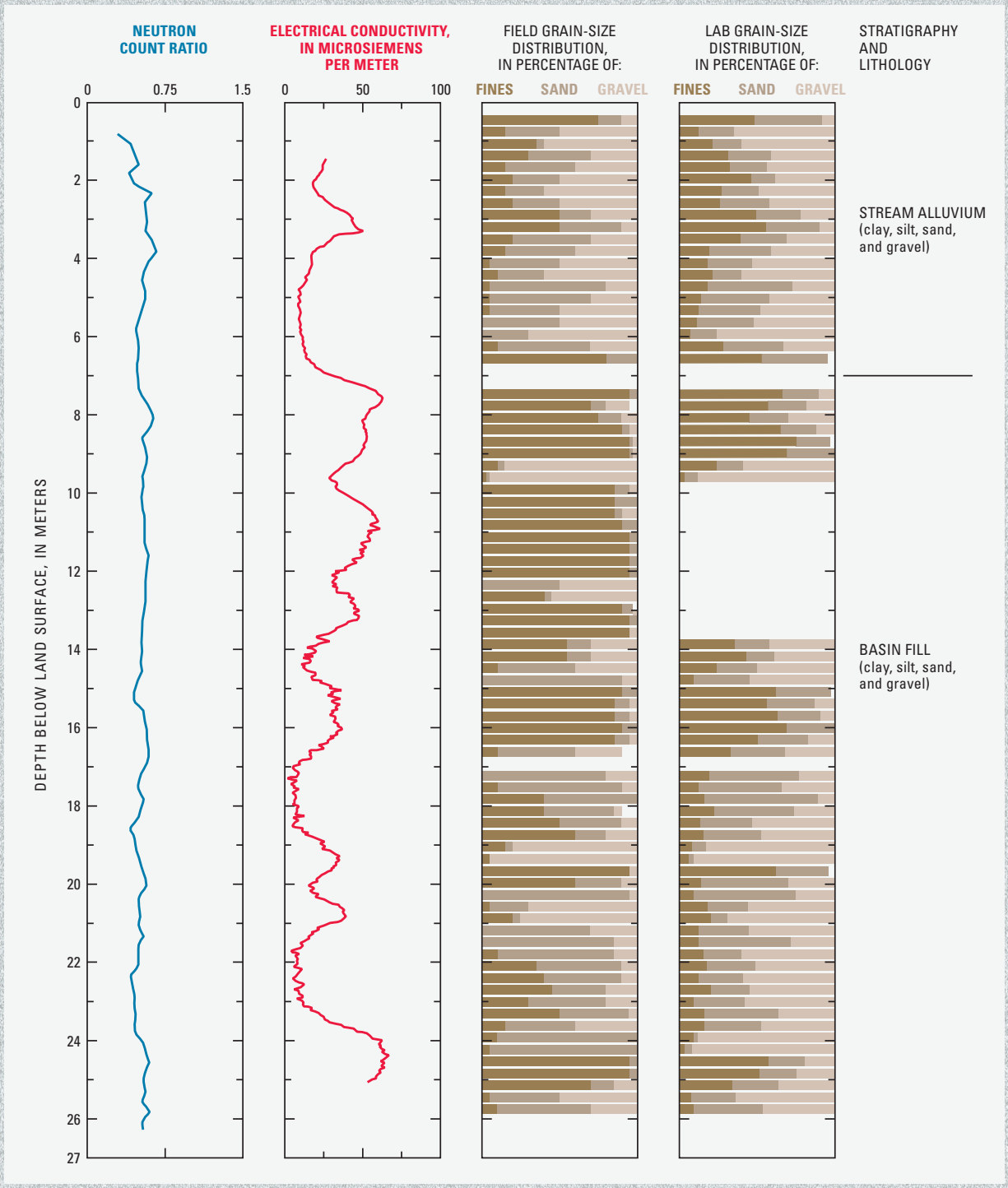

Figure 26. Neutron soil log, electrical conductivity, field and lab grain-size distribution (GSD), stratigraphy and lithology, Banning Creek, Upper San Pedro Basin, southeastern Ariz.

ing relatively low clay contents at 23 meters depth.

All electrical conductivity methods suffer from lack of uniqueness in distinguishing among lithologic, temperature, and pore water salinity. As described above, these confounding factors are accounted for in this study through uniformly low pore water salinity and the combined use of EMI and neutron logs. However, lack of depth resolution remains as a primary limitation on using EMI alone for identifying subsurface structure. This arises due to the relatively large sample volume of the instrument, evident in the EMI response to the 0.3-m thick clay layer located 20 meters below the surface. The EMI response shows a double peak that spans a depth interval of approximately three meters. The double peak is caused by the relatively high sensitivity of the instrument near the transmitting and receiving coils, which are separated by 0.5 meters vertically in the borehole. This instrument response places a limitation on the achievable spatial resolution. The neutron log, as a result of a smaller sample volume, provides higher resolution than the EMI log.

Woodcutter's Wash is also incised (about 6 m) and ephemeral with a sandy channel bottom and outcrops of caliche both up- and downstream of the borehole. Data gathered at Woodcutter's Wash demonstrate the utility of combining EMI and neutron logs (fig. 27). Unlike the Banning Creek logs, the neutron probe counts vary strongly with depth. This is especially apparent at a depth of seven meters, where neutron counts drop significantly while the measured EC remains high. The neutron response indicates that the region has a low volumetric water content. Assuming that pore water electrical conductivity (EC) does not vary significantly with depth, the high EC in this region could indicate that the clay content is higher than the surrounding regions. The elevated clay content would offset the reduction in EC associated with the lower water content. This could be associated with water ponding above the low water content region and the change in lithology below this region. The change in lithology is supported by the laboratory grain size analysis, which indicates that the deepest cuttings (from about 9 m) contain significantly less clay than the material above, possibly indicating the presence of a capillary barrier. However, it is difficult to infer the soil physical property distribution on the basis of one set of cuttings and geophysical logs. Additional laboratory analyses for grain size distribution and water content would result in a better understanding of the spatial variations in these properties. This underscores the fact that geophysical logs are often most useful as a screening tool for identifying regions in which the drill cuttings should be examined closely to interpret subsurface structure.

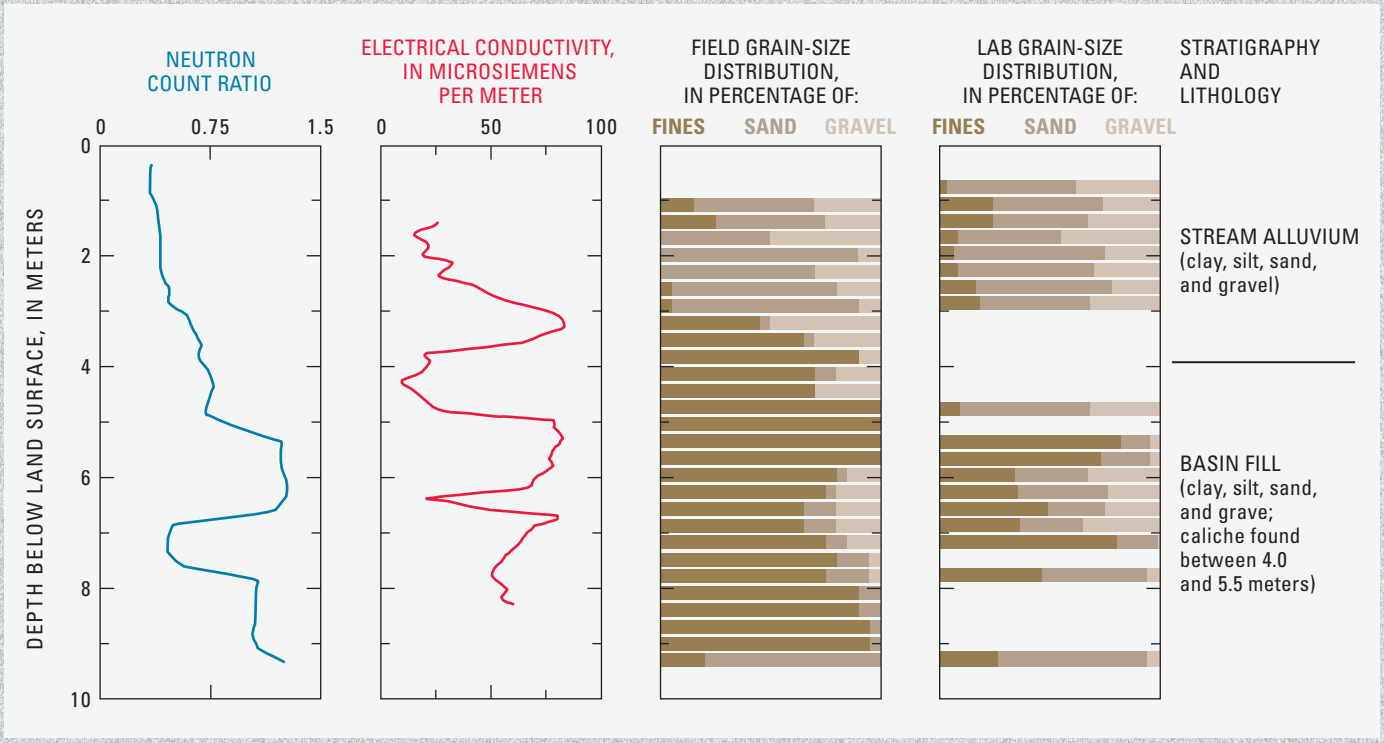

Figure 27. Neutron soil log, electrical conductivity, field and lab grain-size distribution (GSD), stratigraphy and lithology, Woodcutter's Wash, Upper San Pedro Basin, southeastern Ariz.

References Cited

Archie, G.E., 1942, The electrical resistivity log as an aid to determining some reservoir characteristics: Transactions of the American Institute of Mining and Metallurgical Engineers, v. 146, p. 389–409.

Binley, A., Winship, P., Middleton, R., Pokar, M., and West, J., 2001, High resolution characterization of vadose zone dynamics using cross-borehole radar: Water Resources Research, v. 37, no. 11, p. 2639–2652.

Binley, A., Cassiani, G., Middleton, R., and Winship, P., 2002, Vadose zone model parameterisation using cross-borehole radar and resistivity imaging: Journal of Hydrology, v. 267, nos. 3–4, p. 147–159.

Binley, A., Winship, P., West, L.J., Pokar, M., and Middleton, R., 2002, Seasonal variation of moisture content in unsaturated sandstone inferred from borehole radar and resistivity profiles, Journal of Hydrology, v. 267, nos. 3–4, p. 160–172.

Birch, F., 1966, Compressibility, elastic constants, *in* Clark, S.P., ed., Handbook of physical constants: Geological Society of America Memoir 97, p. 97–173.

Blasch, K.W., 2003, Streamflow timing and estimation of infiltration rates in and ephemeral stream channel using variably saturated heat and fluid transport methods: Tucson, University of Arizona, Ph.D. dissertation, 204 p.

Callegary, J.B., Ferré, T.P.A., and Groom, R.W., 2007, Vertical spatial sensitivity and exploration depth of low-induction-number electromagnetic-induction instruments: Vadose Zone Journal, v. 6, no. 1, p. 158–167, doi:10.2136/vzj2006.0120.

Cook, P.G., and Kilty, S., 1992, A helicopter-borne electromagnetic survey to delineate groundwater recharge rates: Water Resources Research, v. 28, p. 2953–2961.

Dane, J.H., and Topp, G.C., eds., 2002, Methods of soil analysis—Part 4, physical methods: Madison, Wisc., Soil Science Society of America, Book Series no. 5, 1692 p.

Desbrandes, R., and Brace, G., 1985, Encyclopedia of well logging: Houston, Gulf Publishing Company, 584 p.

Flint, A.L., and Flint, L.E., 1994, Spatial distribution of potential near surface moisture flux at Yucca Mountain, *in* Fifth International Conference on High Level Radioactive Waste Management, Las Vegas, Nev., May 22– 26, 1994, Proceedings: La Grange Park, Ill., American Nuclear Society, v. 4, p. 2,352–2,358.

Flint, L.E., and Flint, A.L., 1995, Shallow infiltration processes at Yucca Mountain—Neutron logging data 1984–93: U.S. Geological Survey Water-Resources Investigations Report 95–4035, 46 p.

Flint, A.L., and Flint, L.E., 2000, Near surface infiltration monitoring using neutron moisture logging, Yucca Mountain, Nevada, *in* Looney, B. and Falta, R., eds., Vadose zone science and technology solutions: Columbus, Ohio, Battelle Press, p. 457–474.

Flint, A.L., Flint, L.E., Kwicklis, E.M., Bodvarsson, G.S., and Fabryka-Martin, J.T., 2001, Hydrology of Yucca Mountain: Reviews of Geophysics, v. 39, no. 4, p. 447–470.

Flint, A.L., Flint, L.E., Kwicklis, E.M., Fabryka-Martin, J.T., and Bodvarsson, G.S., 2002, Estimating recharge at Yucca Mountain, Nevada, USA, Comparison of methods: Hydrogeology Journal, v. 10, p. 180–204.

Flint, A.L., Hevesi, J.A., and Flint, L.E., 1996, Conceptual and numerical model of infiltration for the Yucca Mountain area, Nevada: Las Vegas, Nev., U.S. Department of Energy, Milestone Report 3GUI623M, 210 p.

Flint, L.E., Hudson, D.B., and Flint, A.L., 1999, Unsaturated hydraulic parameters using indirect and direct methods: *in* van Genuchten, M. Th., Leij, F. J., and Wu, L. eds., Proceedings of the International Workshop for the Characterization and Measurement of the Hydraulic Properties of Unsaturated Porous Media, Riverside, Calif., October 22–24, 1997: Riverside, U.S. Salinity Laboratory, Agricultural Research Service, U.S. Department of Agriculture, and the Department of Environmental Sciences, University of California, p. 293–302.

Geller, J.T., and Myer, L.R., 1995, Ultrasonic imaging of organic liquid contaminants in unconsolidated porous media: Journal of Contaminant Hydrology, v. 19, no. 3, p. 85–104.

Hevesi, J.A., Flint, A.L., and Flint, L.E., 1994, Verification of a 1-dimensional model for predicting shallow infiltration at Yucca Mountain, *in* Fifth International Conference on High Level Radioactive Waste Management, Las Vegas, Nev., May 22– 26, 1994, Proceedings: La Grange Park, Ill., American Nuclear Society, v. 4, p. 2,323–2,332.

Hignett, C. and Evett, S.R., 2002, Neutron thermalization, *in* Dane, J.H., and Topp, G.C., eds., Methods of soil analysis—Part 4, physical methods: Madison, Wis., Soil Science Society of America, Book Series, Number 5, p. 501–521.

Hoffmann, J.P., Ripich, M.A, and Ellett, K.M., 2002, Characteristics of shallow deposits beneath Rillito Creek, Pima County, Arizona: U.S. Geological Survey Water- Resources Investigations Report 01–4257, 51 p.

Hook, W.R., Ferré, T.P.A., and Livingston, N.J., 2004, The effects of salinity on the accuracy and uncertainty of water content measurement: Soil Science Society of America Journal, v. 68, no. 1, p. 47–56.

Hudson, D.B., Flint, A.L. and Guertal, W.R., 1994, Modeling a ponded infiltration experiment at Yucca Mountain, NV, *in* Fifth International Conference on High Level Radioactive Waste Management, Las Vegas, Nev., May 22– 26, 1994, Proceedings: La Grange Park, Ill., American Nuclear Society, v. 4, p. 2,168–2,174.

Huisman, J.A., Hubbard, S.S., Redman, J.D., and Annan, A.P., 2003, Measuring soil water content with ground penetrating radar, a review: Vadose Zone Journal, v. 2, p. 476–491.

Jackson, M.J. and Tweeton, D.R., 1996, 3DTOM, three-dimensional geophysical tomography: U.S. Geological Survey Open-File Report 2000–456, 84 p.

Jury, W.A., Gardner, W.R., and Gardner, W.H., 1991, Soil physics (5th ed.): New York, John Wiley and Sons, 328 p.

Katz, L.T., 1987, Steady state infiltration processes along the Santa Cruz and Rillito rivers: Tucson, University of Arizona, M.S. thesis, 119 p.

Kearey, P., Brooks, M., and Hill, I., 2002, An introduction to geophysical exploration: Oxford, United Kingdom, Blackwell Science Ltd., 262 p.

Keys, W.S., 1990, Borehole geophysics applied to groundwater investigations: U.S. Geological Survey Techniques of Water-Resources Investigations, book 2, chap. E2, 150 p.

Klenke, J.M., and Flint, A.L., 1991, A collimated neutron tool for soil-water measurements: Soil Science Society of America Journal, v. 55, p. 916–923.

Kohnen, H., 1974, The temperature dependence of seismic waves in ice, Journal of Glaciology, v. 13, no. 6, p. 144–147.

Labo, J.A., and Mentemeier, S.H., 1987, A practical introduction to borehole geophysics: Tulsa, Okla., Society of Exploration Geophysicists, 330 p.

Lucius, J.E., Langer, W.H., and Ellefsen, K.J., 2007, An introduction to using surface geophysics to characterize sand and gravel deposits: U.S. Geological Survey Circular 1310, 33 p.

McKittrick, M.A., 1988, Surficial geologic maps of the Tucson metropolitan area: Arizona Geological Survey Open-File Report 88–18 [12 maps; 6 p. text], scale 1:24,000.

NRC (National Research Council) Committee on the Review of the Hanford Site's Environmental Remediation Science and Technology Plan, 2001, Science and technology for environmental cleanup at Hanford: Washington, D.C., The National Academies Press, 192 p.

Or, D., and Wraith, J.M., 1999, Temperature effects on soil bulk dielectric permittivity measured by time domain reflectometry, a physical model: Water Resources Research, v. 35, no. 2, p. 371–383

Patnode, H.W., and Wyllie, M.R.J., 1950, The electrical resistivity log as an aid to determining some reservoir characteristics: Transactions of the American Institute of Mining and Metallurgical Engineers, v. 189, p. 47–52.

Phillips, F.M., 1994. Environmental tracers for water movement in desert soils of the American Southwest: Soil Science Society of America Journal, v. 58, p. 14–24.

Pokar, M., West, L.J., Winship, P., and Binley, A.M., 2001, Estimating petrophysical data from borehole geophysics, *in* Symposium on the Applications of Geophysics to Engineering and Environmental Problems (SAGEEP2001), Proceedings: Denver, Colo., Environmental and Engineering Geophysical Society (CD-ROM).

Reynolds, J.M., 1997, An introduction to applied and environmental geophysics: New York, John Wiley and Sons, 796 p.

Robinson, D.A., Jones, S.B., Wraith, J.M., Or, D., and Friedman, S.P., 2003, A review of advances in dielectric and electrical conductivity measurement in soils using time domain reflectometry: Vadose Zone Journal, v. 2, p. 444–475.

Rubin, Y., and Hubbard, S.S., eds., 2005, Hydrogeophysics: Dordrecht, Netherlands, Kluwer, Water Science and Technology Library, v. 50, 523 p.

Scanlon, B.R., 1991, Evaluation of moisture flux from chloride data in desert soils: Journal of Hydrology, v. 128, no. 1–4, p. 137–156.

Scanlon, B.R., and Goldsmith, R. S., 1997, Field study of spatial variability in unsaturated flow beneath and adjacent to playas: Water Resources Research, v. 33, p. 2239–2252.

Scanlon, B.R., Paine, J.G., and Goldsmith, R. S., 1999, Evaluation of electromagnetic induction as a reconnaissance technique to characterize unsaturated flow in an arid setting: Ground Water v. 37, p. 296–304.

Telford, W.M., Geldart, L.P., and Sheriff, R.E., 1990, Applied geophysics (2nd ed.): Cambridge, United Kingdom, Cambridge University Press, 770 p.

Topp, G.C., Davis, J.L., and Annan, A.P., 1980, Electromagnetic determination of soil water content—measurement in coaxial transmission lines: Water Resources Research, v. 16, p. 574–582.

Turner, S.F., 1943, Ground-water resources of the Santa Cruz Basin, Arizona: Tucson, Ariz., United States Department of the Interior, Geological Survey [not part of a formal publication series], OCLC no. ocm04835814, 84 p.

Tucson Water, 2000, Annual static water level basic data report, Tucson Basin and Avra Valley, Pima County, Arizona, 1997: City of Tucson Water, Planning, and Engineering Division.

Tyler, S.W., Chapman, J.B., Conrad, S.H., Hammermeister, D.P., Blout, D.O., Miller, J.J., Sully, M.J., and Ginanni, J.M., 1996, Soil-water flux in the southern Great Basin, United States—temporal and spatial variations over the last 120,000 years: Water Resources Research, v. 32, no. 6, p. 1481–1499.

Waxman, M.H. and Smits, L.J.M., 1968, Electrical conductivities in oil-bearing shaly sands: Society of Petroleum Engineers Journal, v. 8., no. 2, p. 107–122.

West, L.J., Handley, K., Huang, Y., and Pokar, M., 2003, Radar frequency dielectric dispersion in sand and sandstone, implications for determination of moisture content and clay content: Water Resources Research, v. 39, no. 2, p. 1-1–1-12, doi:10.1029/2001WR000923.

Wilson, L.G., DeCook, K.J., and Neuman, S.P., 1980, Regional recharge research for southwest alluvial basins (final report): Tucson, Ariz., Water Resources Research Center, Department of Hydrology and Water Resources, University of Arizona, OCLC no. ocm19659149, 408 p.

Wood, W.W., and Sanford, W.E., 1995, Chemical and isotopic methods for quantifying groundwater recharge in a regional, semiarid environment: Ground Water, v. 33, p. 458–468.

Yaramanci, U., Lange, G., and Knödel, K., 1999, Surface NMR within a geophysical study of an aquifer at Haldensleben (Germany): Geophysical prospecting, v. 47, p. 923–943.

Yeh, T.-C. J., and Simunek, J., 2002, Stochastic fusion of information for characterizing and monitoring the vadose zone: Vadose Zone Journal, v. 1, p. 207–221.